Attachment 3: Responses to NRC RAIs Specific to WCAP-17788, Volume 1 Supporting the Closure of GSI-191 (PA-SEE-1090) and Mark-ups to WCAP-17788, Volume 1 NON-PROPRIETARY Attachment

The RAIs addressed herein were provided to the Pressurized Water Reactor Owners Group (PWROG) via the following documents:

NRC Correspondence, "Request for Additional Information RE: Pressurized Water Reactor Owners Group Topical Report WCAP-17788, 'Comprehensive Analysis and Test Program for GSI-191 Closure,'" August 2016, ADAMS Accession No. ML16102A357.

RAI-3.4

The example summarized in Table 7-1 of the supplement to Volume 1 (Attachment 1 to WCAP-17788-P) assumes that recirculation begins at 45 minutes. Is this a bounding assumption? Historically, it is assumed that sump recirculation begins at 20 minutes for limiting cases. How do the results of the evaluation change if it is assumed that recirculation starts at 20 minutes?

Response

As described in Table 7-1 of the supplement to WCAP-17788 Volume 1, the example models the emergency core cooling system (ECCS) performance assuming an active failure of a train of safety injection. As such, the injection phase of the accident transient is extended with time, and the 45 minute sump switchover time does not bound the earliest possible sump switchover time that could occur for this plant.

The purpose of the example summarized in Table 7-1 of the supplement to WCAP-17788 Volume 1 is to demonstrate the flow patterns expected at the core inlet following a large cold leg LOCA. After complete core quench, the example shows a strong circulation pattern at the core inlet with upflow in the higher power assemblies in the central region of the core and downflow in the lower power assemblies around the core periphery. As the transient progresses, and decay heat reduces, circulation at the core inlet tends to decay and the flow distribution becomes more uniform with less downflow at the periphery of the core inlet. Since it is expected that areas of the core inlet experiencing downflow will not collect debris, assuming a later debris arrive time (i.e., a later sump switchover time) could lead to a higher fraction of the core inlet forming a debris bed. For this reason, the example summarized in Table 7-1 of the supplement to WCAP-17788 Volume 1 applies a late entry into sump recirculation for a large break LOCA to delay the arrival of debris. This is a realistic entry into sump recirculation when failure of a train of safety injection is considered.

The expected behavior following an earlier entry into sump recirculation can be inferred from the result of the evaluation. When transfer to sump recirculation occurs, there is little change in the core inlet flow distribution. The higher power assemblies are experiencing predominately upflow, while the peripheral assemblies are experiencing predominately downflow. If the transfer to sump recirculation were to occur at 20 minutes post-LOCA, the core inlet flow distribution is also not expected to change significantly. A 20 minute sump switchover time would require two trains of ECCS to be functioning, which would result in more flow to the reactor coolant system (RCS). However, since this example considers a large CLB, the amount of ECCS flow reaching the core inlet is still only that required to replace boil-off (ECCS flow in excess of boil-off spills from the break). At 20 minutes post-LOCA, the circulation pattern at the core inlet is stronger with more downflow. As a result, the fraction of the core inlet expected to collect debris would be smaller.

Based on the above discussion, it is not necessary to bound the earliest sump switchover time. The purpose of the example is to demonstrate the flow patterns at the core inlet under a large CLB scenario, which are not significantly influenced by sump switchover time.

RAI-3.5

Section 7.1.1 of the supplement to Volume 1 states that for regions where flow is upward, debris may collect at the core inlet.

a. As the debris collects, will flow shift to other areas of the core inlet or does the pressure differential remain low enough that flow is not significantly affected?

b. How does the evaluation account for the diversion of flow and debris to areas of the core where debris has not collected?

c. Can a relatively uniform debris bed build at the core inlet as flow is redirected to areas of less debris resistance? If so, how would this affect the conclusions of the evaluation?

Response

a. Debris head loss testing, as described in the response to RAI-3.27, shows that the pressure differential (dP) is low such that the flow distribution is not significantly affected.

b. The assessment in Section 7.1.1 of the supplement to WCAP-17788 Volume 1 does not consider diversion of flow and is intended to illustrate the flow condition prior to and during the initial phase of debris arrival.

c. Under these conditions, a uniform debris bed cannot form at the core inlet. As debris begins to arrive, and potentially accumulate on regions of the core inlet with upflow, the dP is not large enough to significantly influence the redirection of flow. As the transient progresses, other processes (e.g., buoyancy-driven convention) will generate secondary flows that preclude formation of a uniform debris bed.

RAI-3.6

Section 7.1.1 of the supplement to Volume 1 states that the quality of the steam exiting the vessel remains low enough to limit the buildup of boron in the core. How was it determined that maintaining steam quality below 0.8 ensures carryover that will adequately limit the buildup of boron solutes in the core? What is the maximum allowable quality that will ensure excessive boron concentrations will not occur? Provide the basis for this value.

Response

The effect of entrainment on core region boric acid concentration can be estimated with a calculation based on a control volume encompassing the lower plenum, core region and upper plenum. Boric acid will come into the control volume through boiloff makeup at the Refueling Water Storage Tank (RWST) or sump boric acid concentration. Boric acid will leave the control volume via entrainment at the core region boric acid concentration. The core region boric acid concentration will stop increasing when:

$$CORE_{BCMAX} = BOILOFF\ MAKEUP_{BC} \times \left[\frac{1}{(1-x)}\right]$$

Where reactor vessel (RV) exit steam quality, x, is defined as:

$$x = \frac{\dot{m}_v}{\dot{m}_v + \dot{m}_l}$$

And,

$\dot{m}_v$ = vapor phase mass flow rate,

$\dot{m}_l$ = liquid phase mass flow rate.

In terms of Entrainment, E:

$$CORE_{BCMAX} = BOILOFF\ MAKEUP_{BC} \times \left[\frac{1}{(E)}\right]$$

Where Entrainment is defined as:

$$E = \frac{\dot{m}_l}{\dot{m}_v + \dot{m}_l}$$

The SKBOR code has the ability to model entrainment out of the core region and therefore SKBOR is a suitable tool for examining the effect on RV exit steam quality on the ultimate core region boric acid concentration. A base model for this study was Case 1 in Table 7-2 from Section 7.1.1.3 of the supplement to WCAP-17788, Volume 1.

Starting with Case 1, a series of SKBOR runs were made with various levels of constant entrainment throughout the transient. For these cases, the boiloff makeup was assumed to be at a boron concentration of 2500 ppm (actual sump boron concentrations would be much lower). Table RAI-3.6-1 and Figure RAI-3.6-1 show the results of these runs. The results show that 95% RV exit steam quality (5% entrainment) will limit the core region's boric acid concentration to a level below the boric acid solubility

limit of 29.27 wt% at 14.7 psia. As expected, the SKBOR results closely match theoretical limit calculated by the above equations.

The calculational mixing volume will affect the initial rate of buildup of boric acid in the core region, but will not significantly affect the ultimate limit for the core region boric acid concentration. This is demonstrated in Figure RAI-3.6-2 where the 90% RV exit quality case was rerun with a 25% reduction in the lower plenum and core region mixing volume. Figure RAI-3.6-2 demonstrates that when the core region boric acid concentration is controlled by liquid entrainment out of the reactor vessel, the core region mixing volume is not a factor.

While the ultimate limit for the core region boric acid concentration is controlled by the longer term RV exit steam quality, early entrainment will significantly delay the buildup of boric acid. This is demonstrated in a case where the long term RV exit steam quality of 98% was decreased to 96% at 50,000 seconds, 94% at 10,000 seconds, and 92% at 1000 seconds. This schedule for early entrainment extended the time to reach the boric acid solubility limit from 8 ½ hours to 20 hours when compared to the constant 98% constant RV exit steam quality case, as shown in Figure RAI-3.6-3.

Results from this sensitivity study justify the statement made in Section 7.1.1 of the supplement to Volume 1 that the quality of the steam exiting the vessel remains low enough to limit the buildup of boron in the core, because it is shown that a steam quality of 80% results in a maximum theoretical boron solute concentration build-up of less than 7.2 wt% (Case 10, Table RAI-3.6-1). Steam qualities below 80% will result in a lower concentration build-up. The maximum allowable quality that will ensure excessive boron concentrations will not occur is approximately 95% (Case 6, Table RAI-3.6-1) for a boric acid solubility limit of 29.27 wt% at 14.7 psia.

Table RAI-3.6-1 Entrainment Sensitivity Study

Case	Steam Quality	48 hr BAC wt%	Theoretical Max (wt%) =2500*(1/(100-x))/1748.4*100	29.27 wt% HLSO Time (hr)
1	100	> 100	> 100	6.10
2	99	74.19	> 100	7.22
3	98	55.20	71.49	8.93
4	97	42.43	47.66	11.95
5	96	33.75	35.75	19.36
6	95	27.71	28.60	NA
7	93	20.15	20.43	NA
8	90	14.19	14.30	NA
9	85	9.49	9.53	NA
10	80	7.13	7.15	NA

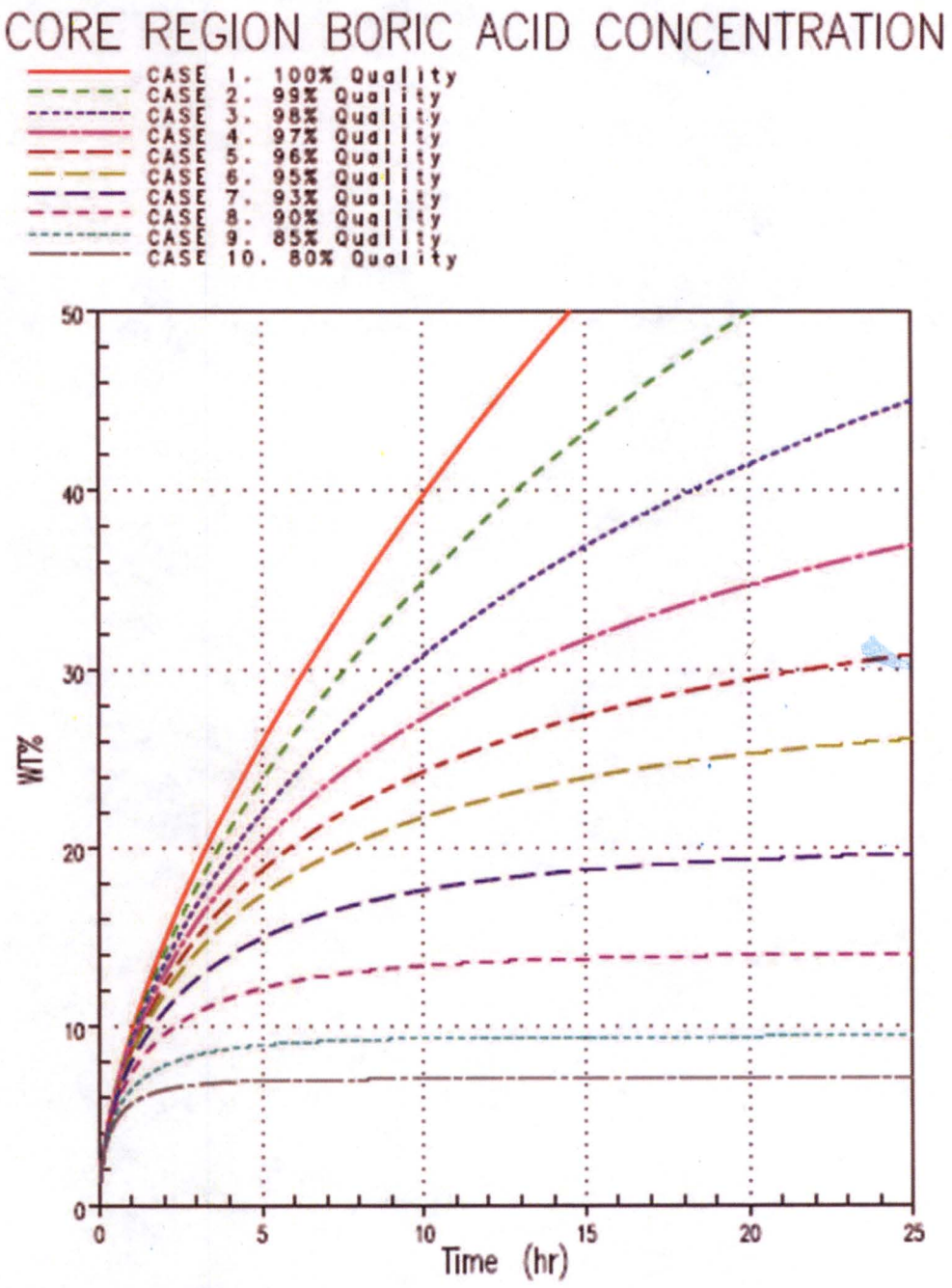

Figure RAI-3.6-1 Effect of Entrainment on Core Region Boric Acid Concentration

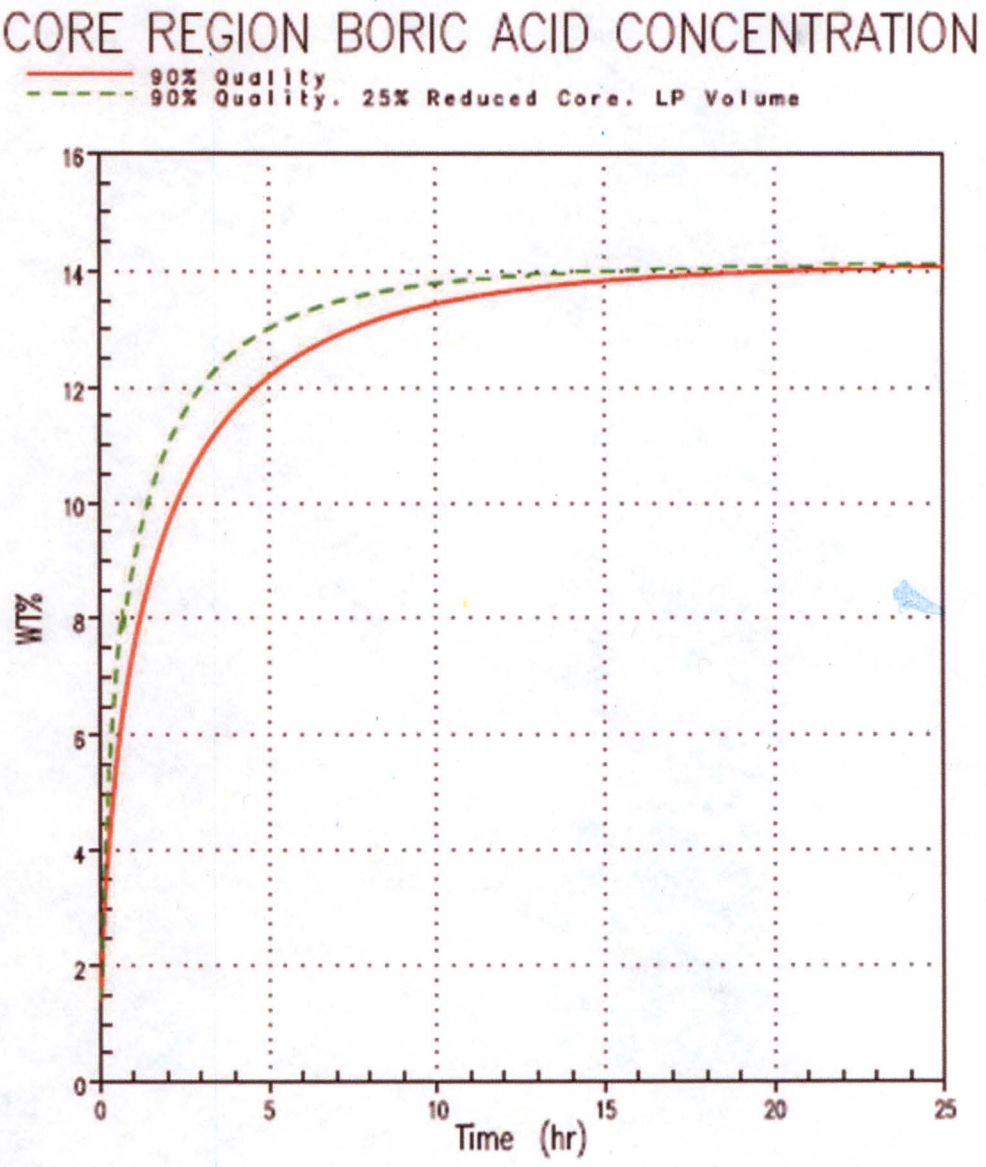

Figure RAI-3.6-2 Effect of Reduced Mixing Volume on Core Region Boric Acid Concentration

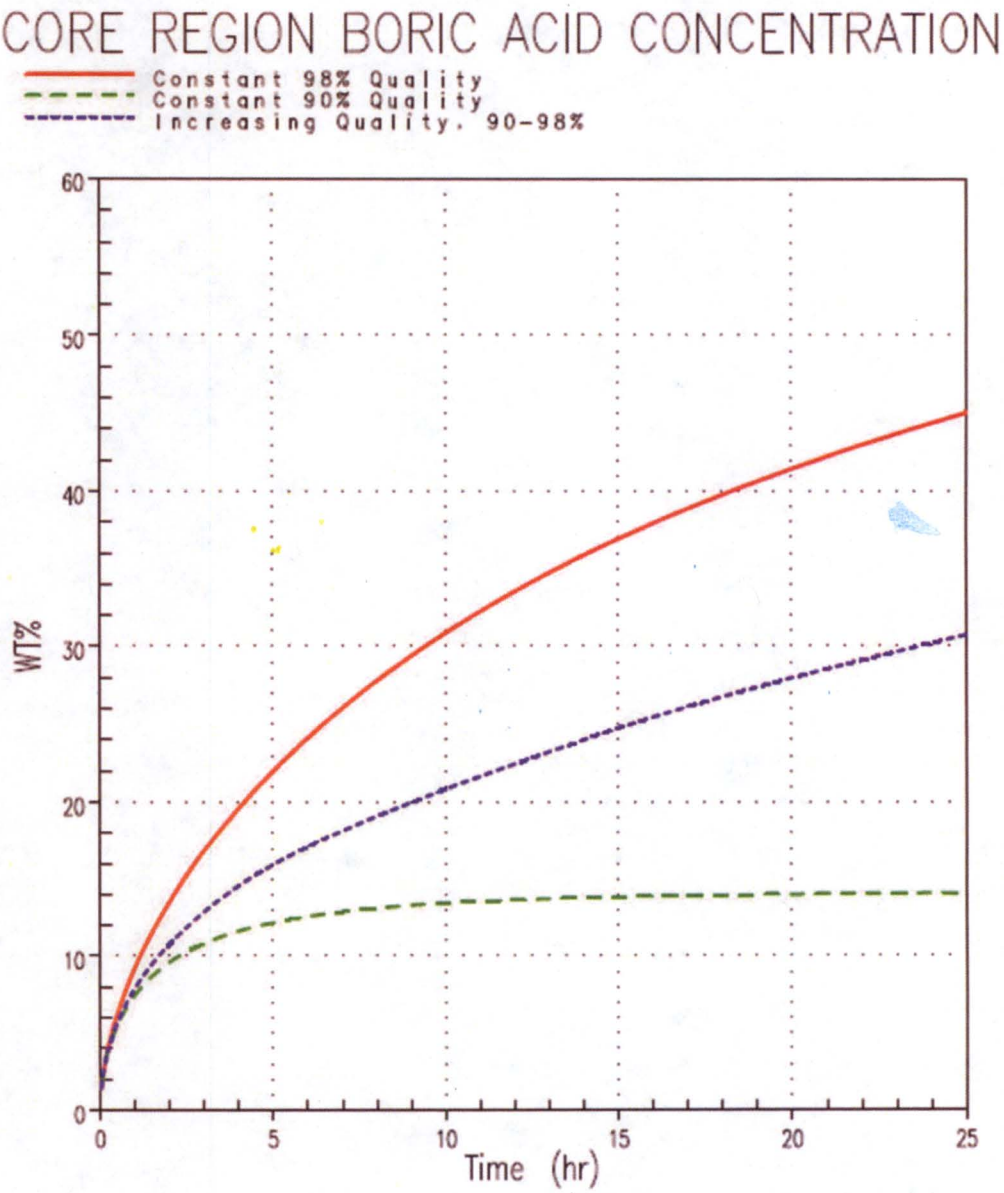

Figure RAI-3.6-3 Effect of Early Entrainment on Core Region Boric Acid Concentration

RAI-3.7

In Figure 7-5 of the supplement to Volume 1, the exit steam quality does not appear to increase significantly at 45 minutes as might be expected when flow to the core is stopped for 2 minutes during swapover. Also, after swapover, the exit quality might be expected to be higher because the temperature of the coolant being injected to the core is assumed to be higher. Discuss the trend in exit quality with respect to these observations. Will these results be used as justification for crediting entrainment?

Response

Prior to sump switchover the exit steam quality is increasing because the steaming rate is decreasing as the decay heat drops. Reduced steaming rates lead to less liquid entrainment and reduced liquid carryover from the reactor vessel into the broken loop hot leg. By the time sump switchover occurs the downcomer has had enough time to fill and the collapsed liquid level is near the cold leg elevation, which is approximately 7 ft above the top of the active fuel. As such, the core mixture level remains above the top of the active fuel during the two minute interruption since there is enough excess liquid in the downcomer to replace boil-off during the interruption. At 45 minutes the steaming rate is approximately 50 lbm/s. If this boiling rate continues for 2 minutes, approximately 100 ft^3 of liquid is removed from the core. The downcomer annulus has a flow area of approximately 30 ft^2. Assuming 100 ft^3 of liquid is removed from the core due to boiling; the downcomer liquid level would reduce by roughly 3 ft, which is still well above the top of the active fuel. For this reason, the exit steam quality is not expected to significantly increase during the two minute interruption. Note that the exit steam quality does increase slightly during the two minute interruption.

During sump switchover the ECCS coolant temperature is increased from 68°F to 150°F. The increase in ECCS coolant temperature increases the enthalpy of liquid entering the core, which increases boiling. Increased boiling produces a higher two-phase mixture level swell, which increases the liquid inventory in the upper plenum region. As such, liquid carryover into the broken loop hot leg increases. Since exit quality is defined as the ratio of vapor mass flow to total mass flow (vapor phase plus liquid phase), an increase in liquid carryover causes the exit quality to decrease.

Licensing basis boric acid precipitation (BAP) analyses currently do not credit liquid carryover into the broken loop hot-side piping. Although the results presented in Section 7.1.1 of the supplement to WCAP-17788 Volume 1 demonstrate that liquid carryover occurs, at least early in the transient, these results are not presented as justification for crediting liquid carryover (entrainment) in licensing basis analyses. These results are used to support the SKBOR sensitivity studies documented in Section 7.1.1.3 of the supplement to WCAP-17788 Volume 1. Specifically, sensitivity Case Nos. 6 and 7 which delay the accumulation start time consistent with the expected effect that liquid carryover will delay the accumulation of boron in the inner reactor vessel. See the response to RAI 3.9 for more discussion.

RAI-3.8

Section 7.1.1.1 of the supplement to Volume 1 discusses the results of the brine test program. The section states that the head loss across the debris bed at the core inlet was maintained very low, even with equivalent fiber loading of 22.5 grams of fiber per fuel assembly (g/FA). The stated pressure drop was about an order of magnitude lower than non-chemical results obtained during testing under cold-leg conditions with 18 g/FA for the test program included in TR WCAP-16793-P-A, Rev. 2, "Evaluation of Long-term Cooling Considering Particulate, Fibrous and Chemical Debris in the Recirculating Fluid."

a. Why are the head loss results for the brine tests significantly different that those reported in WCAP-16793?
b. Why are the results of the brine test, exclusive of previous testing, applicable to the evaluation in WCAP-17788?
c. Why should the results from prior testing not be considered in conclusions for WCAP-17788?
d. The particulate to fiber ratios used during the tests in WCAP-16793 found that the limiting ratios were different for hot and cold leg flow rates. Do the conditions tested during the brine test program provide adequate assurance that particulate has no effect on the test results?

Response

a. The head loss results from the brine testing are different than the WCAP-16793 cold leg break tests because the test procedures were different. In the brine testing, the largest particulate load resulted in a particulate-to-fiber (p:f) ratio of [ ]^{a,c} Test CIB30 from the WCAP-16793 test program was conducted with a p:f ratio of [ ]^{a,c} The particulate loads are comparable; however, because the particulate was allowed to recirculate during the WCAP-16793 test, the final in-bed particulate load prior to the addition of chemical products was higher. Results from both the subscale head loss and the WCAP-16793 test programs demonstrate that [ ]^{a,c} Although there is no way to quantify the in-bed particulate load for Test CIB30, it would be higher than the brine tests conducted with similar particulate loads because the brine testing was conducted with a once-through particulate delivery method.

   A comparison of the tests can be made by examining a once-through condition in Test CIB30. As described in the Westinghouse fuel assembly test report for the WCAP-16793 program (Reference RAI-3.8-1), the cold leg break head loss tests were conducted with a flow rate of 3 gpm. The test facility had a liquid volume of 100 gallons. At the cold leg break flow rates, one liquid turnover in the facility is approximately 33 minutes. The Test CIB30 head loss results from the WCAP-16793 program are shown in Figure 6-12 of Reference RAI-3.8-1. As the figure shows, the first fiber addition is added just before 1.5 hours. After approximately one turnover, the measured head loss is less than [ ]^{a,c} which is comparable to the brine test head loss results conducted with debris loads similar to Test CIB30.

b. The brine tests are not intended to be exclusive of previous testing, as applicable to the evaluations in WCAP-17788. The WCAP-16793 test program cold leg break tests also support the assertion that debris bed formation resulting from [ ]^{a,c} of fibrous debris, or less, will not lead to high head loss prior to the arrival of chemical effects.

c. The results of previous testing can be considered in the conclusions of WCAP-17788. As described in the response to RAI-3.27, the WCAP-16793 results support the conclusions made in WCAP-17788 regarding the cold leg break in-vessel debris limit.

d. Section 7.1.1.1 of the supplement to WCAP-17788, Volume 1 never states that particulate has no effect on the test results. The supplement states that [

]^{a,c} The cold leg break p:f evaluation completed for the WCAP-16793 test program also showed that [

]^{a,c} The WCAP-16793 test program conducted cold leg break tests with the Westinghouse fuel assembly at p:f ratios of [

]^{a,c} in tests CIB29, CIB30, CIB31, CIB32, and CIB33, respectively. The WCAP-16793 cold leg break p:f study determined that a p:f ratio of [ ]^{a,c} resulted in the highest head loss, but all tests measured a head loss of less than [ ]^{a,c} before the addition of chemical products. The increased head loss seen in the WCAP-16793 cold leg break p:f study is also magnified because the particulate was allowed to recirculate, giving the particulate multiple opportunities to capture within the debris bed.

The primary objective of the brine test program was to investigate the effect that a debris bed has on the core-to-lower plenum buoyancy-driven exchange process. The test results demonstrated that increasing the particulate load resulted in a [

]^{a,c}

The effect of increased particulate load on decreasing debris bed stability was also observed in the WCAP-17788 subscale head loss and the WCAP-16793 test programs. The conditions tested in the brine test program provide adequate assurance that [

]^{a,c} This conclusion is consistent with the WCAP-17788 head loss and WCAP-16793 test programs. From the perspective of buoyancy-driven exchange flow, the brine test results demonstrate that the addition of particulate does not significantly change [

]^{a,c}

Reference

RAI-3.8-1 WCAP-17057-P, Revision 1, "GSI-191 Fuel Assembly Test Report for PWROG," September 2011.

RAI-3.9

Section 7.1.1.3 of the supplement to Volume 1 provides the SKBOR case study that was performed to study the sensitivity of boron concentration levels in the core and Lower Plenum (LP). The results of the study are informative, but may not provide realistic or bounding results.

a. Provide a basis for the variables and values chosen for the study.
b. What are realistic assumptions for the core blockage area and accumulation start time for boron?
c. Provide the results of boric acid concentration over time for a case using bounding values for the variables in part a so that the behavior under limiting conditions can be understood.
d. The submittal states that the reactor vessel (RV) steam exit quality remains less than 80% until about 40 minutes after the LOCA. Is this based on a recirculation swapover time of 20 or 45 minutes? What effect does swapover timing have on steam exit quality?

Response

a. The key variables and the basis for their values are summarized in Table RAI-3.9-1. The basis for each value is discussed in detail below.

Table RAI-3.9-1 Summary of key variables and the basis for their value

Key Variable	Basis for Value
Decay Heat	A high decay heat will maximize steaming rate and minimize liquid mixing volume
Mixing Volume	A smaller mixing volume will maximize the accumulation of boron
Boron Source Concentration	A high boron source concentration will maximize the accumulation of boron
Solubility Limit	A low solubility limit will be reached earlier in the transient
Source Coolant Temperature	A saturated coolant temperature will maximize steaming and increase the accumulation rate of boron
Accumulation Start Time	An early accumulation start time will maximize the accumulation rate of boron
Core Blockage Area	A larger fraction of blocked area will reduce the transport rate of boron from the core to the lower plenum

Decay Heat

A larger decay heat value will increase the accumulation rate of boron concentrations in the reactor vessel by increasing the steaming rate and decreasing the liquid mixing volume. The Appendix K decay heat model is selected for the study. The use of Appendix K decay heat in this study is consistent with the decay heat modeling used in current Westinghouse boric acid precipitation licensing basis analyses. Appendix K decay heat bounds all other decay heat models.

Mixing Volume

A smaller mixing volume will increase the accumulation rate of boron in the reactor vessel. In the study, the mixing volume is minimized by:

- Accounting for voiding in the core and upper plenum regions. The void fraction in the upper plenum region is assumed to be equal to the core exit void fraction. The use of Appendix K decay heat and a saturated coolant source maximizes the calculated void fraction.
- Assuming that the two-phase mixture level only extends to the bottom of the hot leg (i.e., no liquid in the upper plenum above the bottom of the hot leg).
- No credit for other regions in the reactor coolant system that contain liquid. The barrel baffle region is not considered part of the mixing volume. The hot leg piping is not considered part of the mixing volume. In the base case, only 50% of the lower plenum volume is credited.

Boron Source Concentration

A higher boron source concentration increases the accumulation rate of boron in the reactor system. A value of 2500 ppm is selected for the study. This value is the maximum value for the water refueling storage tank and accumulators allowed by technical specifications for the plant selected for the study. Also, the source boron concentration is held constant during the analysis, and the effects of boron dilution in the containment sump are not considered. Including the effects of sump dilution would reduce the source concentration over time and decrease the accumulation rate of boron in the reactor vessel.

Solubility Limit

The reactor vessel boron concentration will reach a lower solubility limit earlier in the transient. A solubility limit of 29.27 wt% is selected for the study. This solubility limit is based on an unbuffered boric acid solution at a pressure of 14.7 psia. The presence of buffering agents increases the solubility limit and is not credited. Elevated pressure in the reactor vessel also increases the solubility limit and is not credited.

Source Coolant Temperature

A saturated source coolant temperature will maximize the steaming rate, which increases the accumulation rate of boron in the reactor vessel. A source coolant temperature of 212°F is selected for the study, which corresponds to saturation temperature of pure water at the selected pressure. Subcooling in the source coolant is not credited as the presence of subcooling reduces the steaming rate and increases the effective mixing volume by reducing the void fraction.

Accumulation Start Time

An early accumulation start time will maximize the initial accumulation rate of boron in the reactor vessel since decay heat is highest early in the transient. An early accumulation start time

will decrease the total time required to reach the solubility limit. A 100 second accumulation start time is selected for most of the sensitivities performed in the study. In Case Nos. 6 and 7 the accumulation start time is varied to understand the sensitivity of the results to accumulation start time.

Core Blockage Area

Increasing the fraction of core inlet blockage area will decrease the transport of boron from the core to the lower plenum. The core blockage area is varied as part of the sensitivity study to understand the sensitivity of the results to core blockage area.

b. Given the relatively low state-of-knowledge with regard to core blockage area under large cold leg break conditions, it is difficult to define a realistic fraction of core inlet area that would accumulate debris. This is the reason for performing the sensitivity study. Considering the prototypic system and the conditions that exist under large cold leg break conditions (i.e., low flow velocities and circulation patterns at the core inlet), a significant fraction of the core inlet is not expected to collect debris.

   In this study, the accumulation start time is defined as a means to represent the effects of liquid carryover from the reactor vessel into the hot-side piping. Significant liquid carryover will delay the accumulation of boron in the reactor vessel. Considering the prototypic system and the conditions that exist under large cold leg break conditions, liquid carryover is expected to delay the initial accumulation of boron for hours.

c. The results from Case No. 1 presented in Section 7.1.1.3 of the supplement to WCAP-17788 Volume 1 represent the behavior under limiting conditions. The case applies bounding values for the variables presented in Part a. for the specific type of plant used for the study.

d. As stated in Section 7.1.1.3 of the supplement to WCAP-17788 Volume 1, the statement that the reactor vessel steam exit quality remains less than 80% until about 40 minutes after the LOCA is based on the WCOBRA/TRAC results presented in Section 7.1.1 of the supplement to WCAP-17788 Volume 1. Table 7-1 in the supplement to WCAP-17788 Volume 1 describes the ECCS performance modeled in the WCOBRA/TRAC simulation and shows that the transfer to sump recirculation begins at 45 minutes.

   The timing of sump switchover can impact the steam exit quality because the transfer to sump recirculation can change the ECCS coolant enthalpy. Typically, the ECCS coolant temperature increases following transfer to sump recirculation. As discussed in the response to RAI 3.7, reduced steaming rates lead to less liquid entrainment and reduced liquid carryover from the reactor vessel into the broken loop hot leg. In this case, increasing the coolant enthalpy would increase the steaming rate, and decrease the exit quality.

RAI-3.10

PWROG-15091-P, Section 4.2.2, in describing the selection of the working fluid, provides insights into how the trend of viscosity as a function of mass percent of the working fluid is similar to that of boric acid. Figure 4-2 shows the relationship of concentration versus dynamic viscosity for various combinations of boric acid and buffers compared to the studied working fluids. Potassium Bromide (KBr), the working fluid ultimately chosen for the testing, has an opposite trend as the boric acid results. Describe why KBr was chosen as the working fluid despite this apparent difference.

Response

As discussed in Section 4.2.2 of PWROG-15091-P, Tritton (Reference RAI-3.10-1) states that when the Grashof number (Gr) is large, viscous forces are negligible compared with the buoyancy and inertial forces. Indeed, Tritton states that for small temperature differences (1°C), the Grashof number for water will be on the order of $\sim 10^3$, causing vigorous convection currents to arise. Performing Grashof number calculations for Boric Acid and Potassium Bromide results in values 3 and 2 orders of magnitude greater than that of water, respectively. Therefore, it is shown that discrepancies in viscous effects of the working fluid are negligible and the buoyancy and inertial forces remain dominant.

Additionally, the Froude number (Fr) can be used to reinforce the fact that, so long as the density gradient is equivalent between the salt solution and the boric acid being simulated, the fluid behavior will be similar as well.

Lastly, KBr was also chosen for its practicality. Due to the ability to dispose of KBr in the city sewage system, along with cost, availability, and solute properties at room temperatures to replicate boric acid density gradients, it was selected as the final working fluid.

References

RAI-3.10-1 D. J. Tritton, "Physical Fluid Dynamics," Oxford Science Publications, Second Edition, 1988.

RAI-3.11

For brine tests without debris injection in PWROG-15091-P, the following table summarizes the discussion in Section 9.

Test	Time onset of exchange flow (sec)	Core Concentration	Average Boric Acid (BA) Concentration	Brine source concentration
T012	50	[ ] weight percent (wt%) BA	lower	49 wt% BA
T032	45	[ ] wt% BA	lower	52 wt% BA
T051	55	[ ] wt% BA	higher	52 wt% BA

a. Describe why the core concentration in test T032 is lower than in test T051 at the onset of exchange flow if the brine source concentration is the same between the two tests.

b. Test T032 has a water supply temperature of 60.1 degrees Fahrenheit (°F), which is outside the desired range of 64-72°F. Operating outside of the desired range decreases the accuracy of the conductivity probes. How was this aspect taken into account in the results?

c. Table 9-2 is used to describe the differences in the table above by comparing temperatures in the water supply to the brine supply for all three tests. The submittal states that the lower water injection temperature of T032 makes it more comparable to T051. However, the lower temperature would mean the density differences are increased, and take longer for exchange to occur, but T032 has the earliest onset of exchange flow. Explain why the lower temperature case has the earliest onset of exchange between the core and LP.

d. Explain why the highest core concentration test (T051) has the latest [ ]. Logically, it seems a higher concentration would [ ].

Response

a. To understand the differences between tests T032 and T051, a review of the water and brine supply temperatures is completed. PWROG-15091-P, Table 9-2 lists the liquid temperatures recorded at the beginning of tests T012, T032, and T051. As seen in the table, the water supply temperature in test T032 is lower than the desired range of 64 - 72°F. This temperature range was defined based on the temperature range that was considered for the conductivity probe calibration. Conductivity is dependent on temperature and lower temperatures result in lower measured conductivities. PWROG-15091-P, Figure 9-10 shows the test column inlet and outlet temperatures measured during test T032. As seen in the figure, the inlet temperature is approximately 60°F throughout the test duration, consistent with the water supply temperature.

The test column outlet temperature increases from approximately 60 to 64°F during the test duration, which is consistent with a 66°F injected brine solution mixing with the colder water in the test column. Given the above discussion, the concentrations seen in test T032 are higher than the measurements suggest due to the lower fluid temperature, which if taken into account, would make test T032 more comparable to test T051.

b. As described in Part a., the conductivity probes measure a lower concentration as temperature decreases. The additional uncertainty in the conductivity probe measurement due to operation outside their desired temperature range was not quantified as part of the test program; however, tests conducted with fluid temperatures outside the desired temperature range are identified in PWROG-15091-P, Table 7-1.

c. The submittal states that the lower water injection temperature of T032 makes it more comparable to T051 because the lower temperature results in a lower than expected measured brine concentration. Although it is true that a lower temperature will result in a higher density gradient driven by temperature, the density gradient created by the low injection temperature in test T032 is small compared to density gradients created by variations in brine concentration. For example, the density difference between water at 72°F and 60°F at atmospheric conditions is 0.081 lbm/ft^3. On the other hand, the density difference between a KBr solution with a 0.5 wt% difference is approximately 0.225 lbm/ft^3 under standard conditions. As the example illustrates, the onset of exchange flow is more sensitive to variations in the brine concentration than variations in the fluid temperature. Considering that the conductivity probes have an accuracy of 0.5 wt% or greater, it is not unreasonable to expect that a test with a lower fluid temperature might produce an earlier onset of exchange flow in the testing.

d. First, it needs to be clarified that the tests under consideration in this RAI (tests T012, T032, and T051) were performed without debris. The statement made in the RAI, "Logically, it seems a higher concentration would disrupt the debris bed earlier and initiate exchange flow." is not directly applicable to the tests in question. It would be appropriate to state that a higher core concentration would result in an earlier onset of exchange flow. Although the times reported in the submittal indicate that T051 has the latest onset of exchange flow, it is only 5 and 10 seconds later compared to test T012 and T032, respectively. When the variability in the tests is considered, such as the accuracy of the conductivity probes, a 10 second difference in the onset of exchange flow is reasonable.

RAI-3.12

In Section 10.3 of PWROG-15091-P, results of tests conducted with 15 wt% KBr are presented. These results show that in the AREVA Inc. (AREVA) tests, [ ] and in the Westinghouse Electric Company (Westinghouse) tests, [ ]. It is stated that the core concentration in the AREVA cases is higher, which could lead to these results. It is also stated that the AREVA inlet geometry is [ ].

a. How were differences in core geometry addressed when determining the conditions under which [ ] will occur?
b. Does the core KBr concentration have a higher influence than core geometry on whether or not exchange flow completely stops and on the timing of core breakthrough? Provide a comparison of test results that shows the influence of these factors on the phenomena.

Response

a. Since the conditions under which [ ]^{a,c} occurred were determined experimentally, differences in core geometry were explicitly addressed since prototypic core inlet geometries were used in the tests. The time of [ ]^{a,c} was determined by analyzing the lower plenum solute concentration trend. The [ ]^{a,c} was defined as the time when the lower plenum region solute concentration begins to increase (i.e., exchange flow is reestablished). The conditions under which [ ]^{a,c} occurred were then extracted from the experimental data at the specific time.

b. PWROG-15091-P, Section 10.6 provides results from tests that experienced [ ]^{a,c} based on the Froude number. For the Westinghouse core inlet geometry, the Froude number [ ]^{a,c} For the AREVA core inlet geometry, the Froude number [ ]^{a,c}

The Froude number is calculated using Eq. 4-3 in PWROG-15091-P. Eq. 4-3 shows that the Froude number is a function of superficial velocity, U. Superficial velocity through the bottom nozzle is a function of the flow area. Differences in flow areas between the Westinghouse bottom nozzle and the AREVA lower end fitting (bottom nozzle) were considered when calculating the Froude numbers presented in PWROG-15091-P, Section 10.6. Eq. 4-3 also shows that the Froude number is a function of the core and lower plenum average density, and the density difference, both of which are functions of the core concentration.

The Westinghouse bottom nozzle flow area used in the brine testing is provided in PWROG-15091-P, Table 5-2. The AREVA lower end fitting flow area used in the brine testing is provided in the response to RAI 3.33b. Comparison of the flow areas shows that the AREVA

lower end fitting used in the testing has a flow area that is more than double the Westinghouse bottom nozzle flow area. The superficial velocity through the AREVA lower end fitting will be less than half the superficial velocity through the Westinghouse bottom nozzle for the same volumetric flow rate because the flow area is larger. As such, it is expected that [ ]^{a,c} will occur at a lower core concentration when the AREVA lower end fitting is present for the same volumetric flow rate, debris bed, and lower plenum concentration.

As shown in PWROG-15091-P, Table 10-3, Westinghouse Test T025 and AREVA Test T043 were both conducted with a fiber mass of [ ]^{a,c} and the volumetric flow rates at the time of [ ]^{a,c} were similar; however, the core region concentration at the time of [ ]^{a,c} was approximately 23% lower in the AREVA test compared to the Westinghouse test.

Westinghouse Tests T022 and T024 were both conducted with [ ]^{a,c} of fibrous debris and the same flow conditions. [ ]^{a,c} was observed in both tests. Test T022 was conducted with a KBr source concentration of 10 wt% and Test T024 was conducted with a 15 wt% KBr source concentration. Since Test T024 was conducted with a higher source concentration, the core concentration is expected to be higher, and the time of [ ]^{a,c} is expected to be earlier. PWROG-15091-P, Table 10-3 shows the condition at the time of [ ]^{a,c} for both tests. As expected, the core region concentration is higher in Test T024, and the time that [ ]^{a,c} occurs is earlier. The core inlet flow rate was approximately 9% higher at the time of [ ]^{a,c} in Test T024.

Based on the above discussion and the test comparisons, it can be concluded that the core inlet geometry, because of its effect on superficial velocity, has a stronger influence on determining whether or not exchange flow will stop and the time that [ ]^{a,c} occurs. This can be confirmed by considering the change to the Froude number. If the superficial velocity is decreased by 20%, the Froude number will also decrease by 20%. If the core concentration is increased by 20%, the Froude number will decreased by less than 10%. Since the AREVA lower end fitting has a larger flow area, the superficial velocity is smaller, making this geometry more prone to [ ]^{a,c} Conditions with higher core concentrations also promote [ ]^{a,c} because the potential for exchange flow is increased.

RAI-3.13

The timing of [ ] in Figure 1 0-11 of PWROG-15091-P spans between about [ ]. Explain why the [ ] is so diverse. Include a discussion about whether or not measurement uncertainty was credited in the explanation.

Response

PWROG-15091-P, Figure 10-11 shows average core and lower plenum concentrations from four tests completed using the AREVA lower end fitting. Although all four tests are reported as being performed at the same nominal test conditions, tests T041 and T048 had higher source KBr concentrations, which is why the average core concentrations from these two tests are higher in Figure 10-11. The diversity seen in the results from these four tests can be attributed to [

]^{a,c}

[

]^{a,c}

With regard to measurement uncertainty, the concentration measurements from tests T041 and T048 are less accurate than the measurements made during tests T052 and T054. The response to RAI-3.18 discusses concentration measurement accuracy. However, citing the increased measurement uncertainty in test T041 and T048 is not necessary to explain the behavior in question.

RAI-3.14

In PWROG-15091-P, many brine tests were conducted to understand the effect of particulate on [ ]. Figure 10-8 (tests T036 and T042) shows that particulate delays the timing of [ ]. Figure 10-12 (tests T040 and T049) shows that [ ]. Explain this discrepancy in the results. Justify that the tests conducted without particulate are representative of the behavior that would occur in the plant or state that the results of those tests are not relevant to the conclusions drawn from the testing.

Response

PWROG-15091-P, Figure 11-2 (tests T016 and T020) also shows that the test conducted with particulate debris (T020) resulted in an [ ]^{a,c} compared to the test run without particulate (T016), which is consistent with the behavior shown in PWROG-15091-P, Figure 10-12. Therefore, Test T036 is the only particulate test that did not lead to [ ]^{a,c} when compared to tests conducted at similar conditions without particulate.

The discrepancy in Test T036 is an anomaly and cannot be explained with the available brine testing; although the behavior is likely to be related to debris bed variability. An overall observation from the brine testing was that [

]^{a,c} Additionally, three other tests were completed at the same condition as Test T042; Tests T035, T053, and T055. The average core and lower plenum concentrations from these four tests are shown on PWROG-15091-P, Figure 10-7. As the figure shows, [

]^{a,c} The discrepancy observed in Test T036, and the inability to explain it with absolute certainty, does not invalidate the conclusions drawn from the brine testing.

RAI-3.15

In Figures 7-1 and 7-2 of PWROG-15091-P, it appears that the pressure increases significantly more for the delayed injection tests. Is this an actual result or is Figure 7-1 not showing the extent of the increase? Provide the magnitude of the increase for each test type.

Response

PWROG-15091-P, Figure 7-1 is not showing the extent of the pressure increase. Since the start of the brine injection pump was not controlled by the data acquisition system, the start time of brine injection is not always consistent with the start time of the data acquisition system. In the case of test T029 (Figure 7-1), the brine injection pump was started just prior to the start of the data acquisition system.

The column test pressure was recorded manually in the test procedures prior to starting the brine injection pump. The initial column pressure, prior to brine injection, reported for test T029 is 2.92 psi. Based on PWROG-15091-P, Figure 7-1, the maximum pressure achieved after the start of brine injection is approximately 6.3 psi. The magnitude of pressure difference for test T029 is 3.38 psi.

This pressure difference is comparable to test T021. From PWROG-15091-P, Figure 7.2, the pressure prior to brine injection is approximately 2.2 psi and the maximum pressure after brine injection is approximately 5.4 psi. The magnitude of pressure difference for test T021 is 3.2 psi.

RAI-3.16

At the bottom of Page 10-8 of PWROG-15091-P, verify that the test that had the lowest core region concentration is T052 instead of T054, as stated.

Response

Correct. Test T052 is the test that had the lowest core region concentration.

RAI-3.17

In PWROG-15091-P, what caused the flow rate for brine test T018 shown in Figure 10-10 to decrease so quickly at both around 1,800 seconds and at the end of the test? Was this a planned evolution?

Response

The reduction of flow for test T018 was a planned evolution. Note that in PWROG-15091-P, Table 6-1, the footnote in the table indicates that for test T018 the flow was manually reduced at the end of the test. At approximately 1800 seconds, the flow was manually reduced from 0.5 gpm to 0.25 gpm. At approximately 2500 seconds, the flow was manually stopped, and the test was terminated.

RAI-3.18

Table 5-5 of PWROG-15091-P shows the conductivity probe accuracy. The accuracy after Calibration 2 is significantly higher for all probes. Why is the accuracy much higher after Calibration 2? How was the accuracy accounted for in the overall results of the evaluation?

Response

A summary of the conductivity probe calibration is provided in Table RAI-3.18-1. Calibration of the probes was completed using 500 mL standards at KBr concentrations of 1, 5, 10, 15, and 20 wt%. As shown in Table RAI-3.18-1, an original five-point calibration was performed on 2/10/2015 prior to shakedown testing. On 3/2/2015, a three-point calibration check was completed. The check confirmed that the original calibrations were still valid. Then, on 4/8/2015, it was determined that the probe signal had drifted and a recalibration was performed. Finally, at the conclusion of testing on 4/15/2015, a post-calibration was performed which confirmed that the recalibration completed on 4/8/2015 remained valid.

Since multiple calibrations were performed during the duration of the test program, multiple calibration curves, with different accuracies, are needed to reduce the entire dataset. For each conductivity probe, three calibration curves are needed to reduce the data. The raw signal calibration values collected at a given standard concentration were used to create third-order polynomial curve fits that correlate the raw output signal to wt% KBr. The correlation was then applied to the experimental calibration data to determine the accuracy of each calibration curve by comparing the concentration standards to those predicted by the correlation.

As an example, the first calibration curve from probe CP2 is shown in Figure RAI-3.18-1. This calibration curve was generated using the calibration data from 2/10/2015 and 3/2/2015 and is valid for tests performed over that time period. The tests performed over that time period were the shakedown tests and tests T012 – T021. Similar curves were generated for the other seven probes.

The second calibration curve for probe CP2 is shown in Figure RAI-3.18-2. This calibration curve was generated using data from 2/10/2015, 3/2/2015, and 4/14/2015 and is valid for tests performed from 3/3/2015 to 4/7/2015. The tests performed over that time period were T022 – T051. Since drift occurred over this time period, the original calibration data was averaged with calibration data collected after the drift was identified. Because of this, the accuracy of the conductivity probes is significantly less compared to the other sets of calibration curves. Similar curves were generated for the other seven probes.

The third calibration curve for probe CP2 is shown in Figure RAI-3.18-3. This calibration curve was generated using data from 4/8/2015 through 4/15/2015 and is valid for tests completed over that time period. The tests performed over that time period were T052 – T055. Similar curves were generated for the other seven probes.

As described in PWROG-15091-P, Section 7.8, the brine concentrations are volume-averaged based on test geometry to determine a core region and lower plenum region average concentration. PWROG-15091-P, Figure 5-14 shows the axial locations of the conductivity probes as well as the control volumes that will be used to perform the volume averaging. The physical volumes of each control volume are calculated based on the physical dimensions of the test column. Probes CP3, CP6, and CP7 were used to calculate the core region average concentration and probes CP5, CP1, CP2, and CP4 were used to calculate the lower plenum volume average concentration.

The conductivity probe accuracy was used to calculate the uncertainty in the volume-averaged concentrations by taking the partial derivative of the volume average with respect to each variable, multiplication with the accuracy in that variable, and addition of these individual terms in quadrature. PWROG-15091-P, Equation 7-8 and Equation 7-9 perform this operation for the lower plenum and core regions, respectively. As such, the accuracy of each conductivity probe is accounted for in the uncertainty of the volume-average lower plenum and core region concentrations.

Table RAI-3.18-1 Summary of Conductivity Probe Calibration

Calibration Date	Description	Number of Calibration Points	Calibration Range (wt% KBr)
2/10/2015	Original calibration of probes CP1 – CP8	5	0 – 20
3/2/2015	Calibration check of probes CP1 – CP8	3	0 – 10
3/17/2015	Original calibration of probe CP1a (CP1 replacement)	5	0 – 20
4/8/2015	Recalibration of probes CP1a – CP8	5	0 – 20
4/14/2015	Calibration check of probe CP8	4	0 – 15
4/15/2015	Post-calibration of probes CP1a – CP8	4	0 – 15

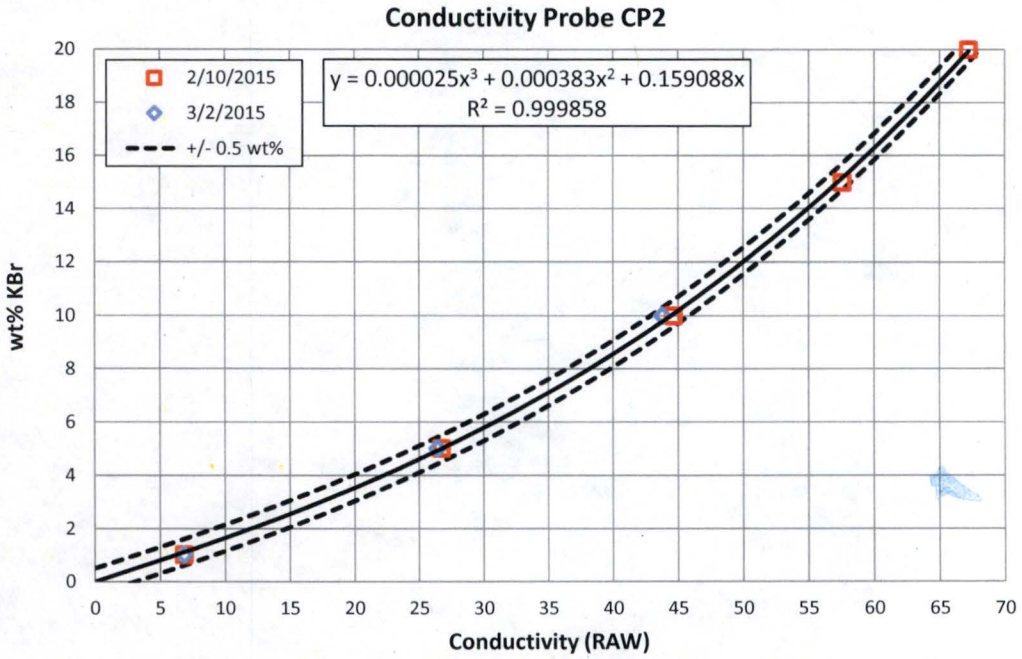

Figure RAI-3.18-1 Conductivity Probe CP2 Calibration Curve for Experiments Conducted between 2/10/2015 and 3/2/2015

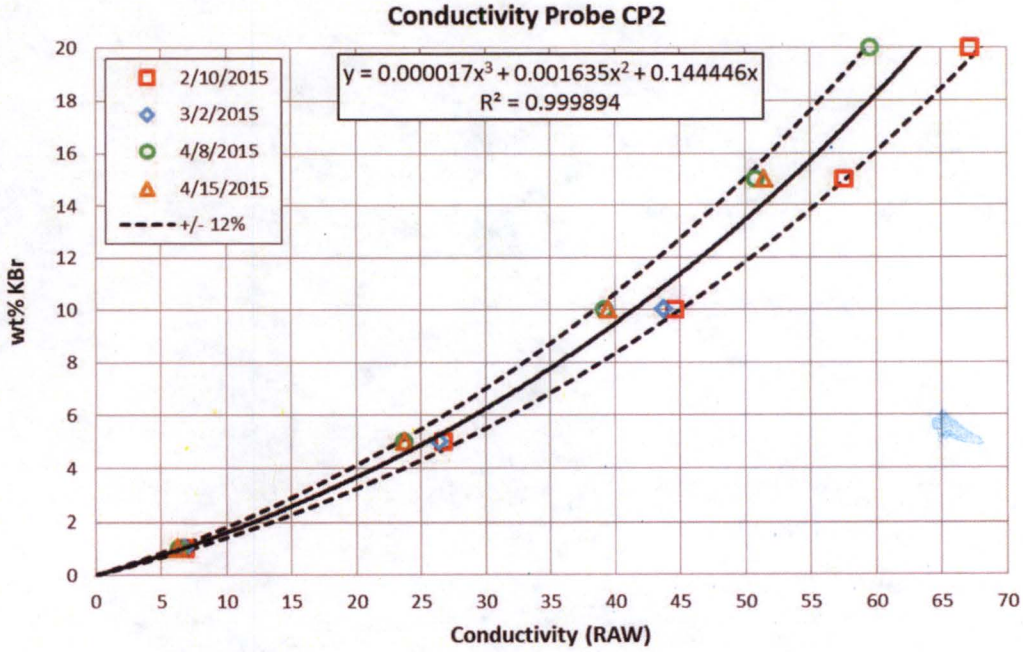

Figure RAI-3.18-2 Conductivity Probe CP2 Calibration Curve for Experiments Conducted between 3/3/2015 and 4/7/2015

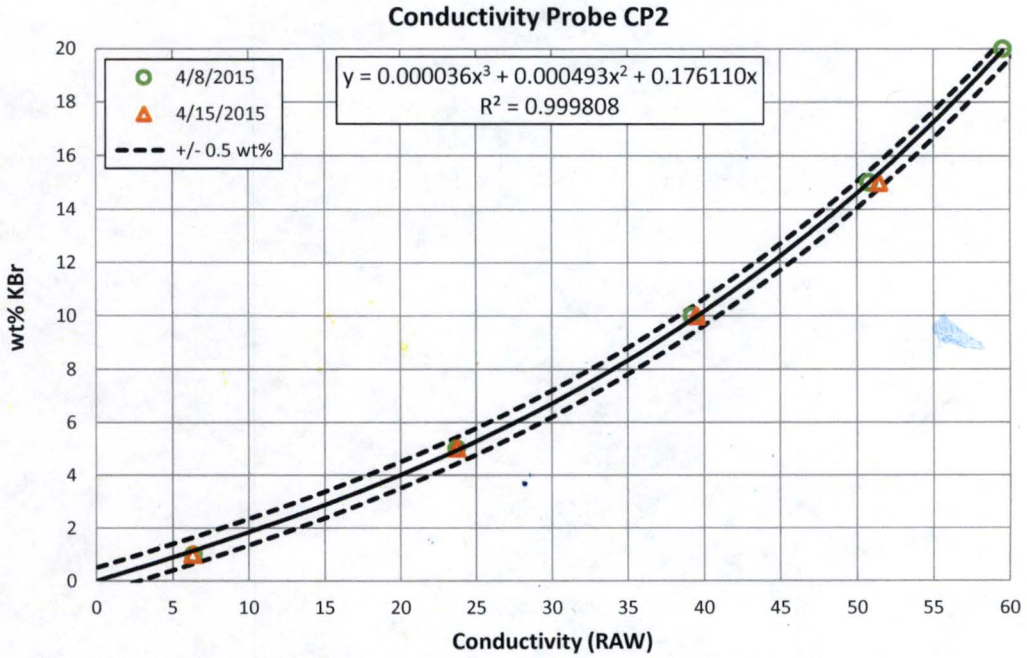

Figure RAI-3.18-3 Conductivity Probe CP2 Calibration Curve for Experiments Conducted between 4/8/2015 and 4/15/2015

RAI-3.19

In brine test T022 of PWROG-15091-P, [
]. Can this result be used to predict [ ] for this concentration, debris loading, and core inlet geometry?

Response

Yes. As stated in Section 10.2 of PWROG-15091-P, [ ]^{a,c} occurred in tests T022 and T018 at similar flow conditions (i.e., upwards flow), as well as similar density gradients. Therefore, these results can be used to predict [ ]^{a,c} for this concentration, debris loading, and core inlet geometry.

RAI-3.20

Were any brine tests with delayed brine injection in PWROG-15091-P run using the AREVA core inlet geometry? If not, how can the Westinghouse results for tests with delayed brine injection be confidently used for making conclusions with the AREVA inlet geometries?

Response

No delayed-injection tests were run with the AREVA inlet geometry. Test results from the delayed-injection tests using Westinghouse geometry were not used to make conclusions about expected performance with regard to AREVA geometry.

In both instances (simultaneous and delayed injection), the test results demonstrate that [

]^{a,c}

RAI-3.21

In PWROG-15091-P, how does the scaling and operational parameters of the brine test rig affect the results of the testing as compared to the plant condition? For example, how does the head of higher density solution in the core compare to the head of higher density solution in the test? In the core there is significant voiding while in the test the assembly is not full height. Justify that the test results or observations from the test can be applied to the plant condition considering the physical differences between the test facility and plant conditions.

Response

Global natural circulation through the reactor vessel depends largely upon the single-phase and two-phase gravity head. As the brine test facility is a reduced height adiabatic facility, these parameters are not well-preserved and the global natural circulation in the brine facility would be smaller than the circulation expected in the plant because of the reduced height. However, as described in PWROG-15091-P, Section 3, buoyancy-driven exchange flow between two regions separated by a horizontal partition is governed by the local geometry of the partition; in this case, the core inlet. As the brine test facility utilized prototypic core inlet geometry, the buoyancy-driven exchange flow between the core and lower plenum would be well-preserved.

It is also important to consider differences in fluid properties between brine and boric acid. The Froude number can be used to predict the onset of buoyancy-driven exchange flow by providing the relative importance of inertia to buoyancy forces. The Froude number is a function of the average density between the two fluids in the core and lower plenum and the density gradient between the two regions. This formulation reinforces the fact that so long as the density gradient is equivalent between the brine solution and boric acid, the fluid behavior will be similar. The source concentration of the brine solution used in the brine testing was selected such that the density gradient between the core and lower plenum would be preserved, as compared to actual plant conditions.

RAI-3.27

The supplement to Volume 1 attempts to establish the basis for an in-vessel fiber limit of [ ] for the CLB scenario. Instead of providing a basis for choosing [ ], various aspects are discussed to show why [ ] would not adversely impact Long Term Core Cooling. Testing results from the brine test program and the 3x3 heated rod bundle program are presented to demonstrate that transport between the core and LP will continue in the presence of in-vessel debris without indicating the amount of debris this applies to. Provide a quantitative basis for choosing a debris limit of [ ] for the CLB scenario. Provide justification for why the limit applies to all plant categories in WCAP-17788.

Response

The supplement to WCAP-17788, Volume 1 identifies five items that need to be addressed in order to demonstrate that the CLB in-vessel debris limit will not adversely impact long-term core cooling (LTCC):

1. Debris collection at the core inlet resulting in increased pressure losses through the inner RV such that the two-phase mixture level is reduced below that required to keep the core covered.

2. Debris collection at the core inlet such that the transport of high concentration boron solution from the core to the LP is reduced below that required to maintain adequate Boric Acid Precipitation Control (BAPC).

3. Suspended debris in the liquid-phase within the RV resulting in increased pressure losses through the inner RV due to changes in apparent fluid properties, two-phase flow characteristics, and heat transfer processes.

4. Suspended debris in the liquid-phase within the RV resulting in premature BAP due to a reduction in the two-phase mixture level or liquid inventory, a reduction in liquid carryover, or changes to the precipitation mode or precipitation location.

5. Local collection of debris on spacer grids within the core region resulting in increased frictional resistance through the core region or reduced heat transfer.

With regard to Item 1, head loss testing completed as part of the brine testing demonstrated that the head loss due to debris accumulation at the core inlet under large CLB conditions was significantly low for fibrous debris loads up to [ ]^{a,c} The WCAP-16793-NP-A, Rev. 2 (Reference RAI-3.27-1) head loss test program also showed that the head loss was significantly low under large CLB conditions for fibrous debris loads up to [ ]^{a,c} (See the response to RAI-3.8).

The largest pressure drop measured across the debris bed from these tests (before chemical product addition) was [ ]^{a,c} from test CIB32 (Reference RAI-3.27-2). Under large CLB conditions, the static head in the downcomer is limited by the break elevation, and the available driving head is the difference between the static head in the downcomer and the pressure drop across the core and the broken loop to the break location. Conservative plant calculations show that the available driving head in the

downcomer is greater than 1psi, which is [ ]^{a,c} The discussion in Section 7.1 of the supplement to WCAP-17788, Volume 1 provides the basis for why a continuous debris bed cannot form at the core inlet under large CLB conditions. If a continuous debris bed does not form at the core inlet, the actual core inlet pressure drop across the debris bed would be less than that measured in the testing. However, even without crediting a non-continuous debris bed at the core inlet, the available driving head in the downcomer is large enough to ensure adequate flow reaches the core to replace boil-off and maintain adequate LTCC. As provided in WCAP-16793-NP-A, Rev. 2 (Reference RAI-3.27-1) the head loss test program is applicable to all plant categories in WCAP-17788. As such, the testing shows that Item 1 is addressed for CLB in-vessel debris loads of up to [ ]^{a,c}

With regard to Item 2, the brine testing demonstrated that debris [ ]^{a,c} will occur for fibrous debris loads up to [ ]^{a,c} such that communication between the core and lower plenum will continue. Note that one test using the Westinghouse core inlet geometry was completed using a fibrous debris load of [ ]^{a,c} This test also demonstrated debris [ ]^{a,c} however, the highest fibrous debris loading tested with the AREVA core inlet geometry with brine injection was at [ ]^{a,c} As described in PWROG-15091-P and supplemented by the response to RAI-3.21, the brine test facility preserved the key phenomena related to buoyancy-driven convection, such that the test observations are applicable to all plant categories considered in WCAP-17788. As such, Item 2 can be addressed for CLB in-vessel debris loads of up to [ ]^{a,c} The WCOBRA/TRAC and SKBOR analyses, and the 3x3 testing presented in the supplement to WCAP-17788, Volume 1 provide additional assurance that communication between the core and the lower plenum will continue at the CLB in-vessel debris limit.

With regard to Items 3 and 4, the 3x3 boiling tests documented in WCAP-17360 (Reference RAI-3.27-3) showed that suspended debris did not significantly impact the two-phase flow characteristics or the heat transfer processes. The tests also showed that the two-phase mixture level, and the timing and location of boric acid precipitation were not significantly impacted by the presence of suspended debris. The 3x3 boiling tests were completed with a fibrous debris loading of [ ]^{a,c} From the perspective of the effects of suspended debris, the 3x3 testing supports a CLB in-vessel fibrous debris limit of [ ]^{a,c} As described in WCAP-17788, the key physical phenomena under consideration in the testing are reasonably scaled to prototypic Pressurized Water Reactor (PWR) conditions, making the tests applicable to all plant categories in WCAP-17788. As such, Items 3 and 4 can be addressed for CLB in-vessel debris loads of up to [ ]^{a,c}

With regard to Item 5, WCAP-16793-NP-A, Rev. 2, Section 4.4 (Reference RAI-3.27-1) summarizes cladding heatup calculations performed to demonstrate that localized blockages will not impede LTCC. WCAP-16793-NP-A, Rev. 2 is approved for in-vessel fibrous debris loadings up to 15 g/FA. Sensitivity studies were performed for other PWR fuel designs in WCAP-16793-NP-A, Rev. 2, making the results applicable to all plant categories considered in WCAP-17788 since the same plants were considered in WCAP-16793-NP-A, Rev. 2. The 3x3 boiling tests showed that local debris collection at spacer grid locations was minimized such that resistance due to this local collection would not be significant for

fibrous debris loads up to [ ]^{a,c} As such, Item 5 can be met for CLB in-vessel debris loads of 15 g/FA or greater.

Based on the testing and analysis described above, acceptable fibrous debris limits have been quantified that address each of the five items necessary to demonstrate adequate LTCC. Since all five items need to be addressed, the minimum acceptable quantity of fibrous debris is chosen for the WCAP-17788 CLB in-vessel debris limit; [ ]^{a,c} which is applicable to all plant categories in WCAP-17788.

References

RAI-3.27-1 WCAP-16793-NP-A, Rev. 2, "Evaluation of Long-Term Cooling Considering Particulate, Fibrous and Chemical Debris in the Recirculating Fluid," July 2013.

RAI-3.27-2 WCAP-17057-P, Revision 1, "GSI-191 Fuel Assembly Test Report for PWROG," September 2011.

RAI-3.27-3 WCAP-17360-P/NP, "Small Scale Unbuffered and Buffered Boric Acid Nucleate Boiling Heat Transfer Tests with Sump Debris in a Vertical 3x3 Rod Bundle," May 2012.

RAI-3.28

Section 7 in Volume 1 states that the subscale brine test program documented in PWROG-15091, states that "the testing considered a broad range of conditions prototypic of those expected to occur following a postulated large CLB LOCA." Section 7 explains that the flow rate through the test column was scaled "based on the boil-off rate calculated for prototypic post-LOCA conditions." Specifically, "for tests that had brine injection, the flow rate was reduced during each test consistent with the DH curve" and for tests conducted with debris only (no brine injection) the flow rate was held constant at a value consistent with DH boil-off calculated at 20 minutes post-LOCA. Figure 5-5 in PWROG-15091 shows the two flow curves defined for the brine testing. Figures 7-8, 7-9, 7-10, 8-1, 9-1, and 10-10 show measured flow rates for selected tests. The CLB methodology in Volume 3 will be used to calculate the amount of fiber delivered to the core inlet from the time of initiation of sump recirculation to the time of HL switchover. Provide the following information to assure that the flow rates in the brine testing program are bounding for expected large CLB conditions.

a. Identify the DH model used to scale the test flow curves in Figure 5-5 and clarify whether the uncertainty in the model was accounted for (e.g., using a 1.2 multiplier).
b. Justify that the flow rate through the test column (based on boil-off rate post-LOCA) is bounding for all plant categories in the operating fleet. If it cannot be shown as bounding, why is a plant with a flow rate outside the bounds of the test able to apply the test results?
c. What is the accuracy of the flow rate through the test column?
d. What is the accuracy of the brine injection flow rate?
e. Considering the variability in both the time of initiation of sump recirculation and the time of HL switchover among individual plant units using this methodology, explain how the experimentally attained test flow conditions were prototypic. Specifically, provide justification with regard to plant units that have shorter time of initiation of sump recirculation and/or switchover to HL injection. The concern is that earlier times of initiation of sump recirculation and/or switchover to HL injection will have higher flow rates compared to the test flow rates so the bed break-through may occur in the plant at different times than observed in testing.
f. Volume 3 explains "to allow for uncertainties, the fluid volume entering the fuel is assumed to be 1.2 times the boil-off flow rate requirement based on the decay heat at any given time in the transient starting at recirculation initiation." Explain how the test flow condition in the brine test program accounts for the uncertainty of this parameter.

Response

a. Appendix K decay heat (1.2 times the values for infinite operating time in the ANS 1971 Standard) was used to define the test flow curves.

b. The objective of the brine testing was to determine the condition under which debris [ ]^{a,c} occurs. In the tests, a debris bed was formed for a given brine injection

source concentration. In the tests completed with higher debris loads [ ]^{a,c} Selection of the brine flow control curve was determined based on the plant boil-off rate to ensure that the range of flow rates used in the brine testing were representative of those expected to occur in the prototypic system, and it was not necessary to bound all flow rates in the system at all times.

c. The accuracy of the flow rate through the test column is discussed in the response to RAI-3.29.

d. The accuracy of the brine injection flow rate is discussed in the response to RAI-3.29.

e. As discussed in the response to RAI-3.30, the brine tests cannot be scaled with time. Instead of simulating a transient condition in which the solute concentration in the core region is continually increasing, the strategy taken for the brine testing is to create a series of quasi-steady-state conditions in which buoyancy-driven exchange flow will occur in the subscale facility. For this reason, the time of [ ]^{a,c} will occur at different times in the plant than observed in the testing. The brine testing determines the condition under which debris [ ]^{a,c} is predicted to occur, and it is not necessary to preserve the time scale.

f. There is no direct relationship between what is assumed in Volume 3 and what is used as a boundary condition in the testing. The brine testing determines under what conditions debris [ ]^{a,c} will occur, which is independent of the assumptions made in the Volume 3 methodology.

RAI-3.29

Section 7.4 of PWROG-15091, "Test Column Flow Rates," states that "the outlet flow rate, which is the combination of inlet and brine injection flow rates, is measured during each experiment." The test report lists an accuracy of "0.258% rate" and a range from 0 to 100 gpm for this device.

The maximum main flow rate in all tests was 0.8 gpm equating to 0.8% of the flow meter upper range limit. The minimum flow rate in the tests using Flow Control 1 was [ ] of the flow meter upper range limit and about [ ] in the tests using Flow Control 2. Even with the addition of the brine solution injection flow of 0.5 gpm, the corresponding total flow rates and fractions are [ ]. These measured flow rates represent very small quantities compared to the upper range limit of 100 gpm of the flow meter.

a. Clarify whether the accuracy of the magnetic flow meter provided in Table 5-4 as "0.258% rate" is valid for the entire specified range from 0 to 100 gpm or it is based on the upper range limit of 100 gpm.
b. Provide the accuracy for the brine injection flow rate relative to setting the speed of the positive displacement pump in order "to achieve the prescribed brine injection flow rate of 0.5 gpm."
c. Provide the calculation for the error in the main flow rate used in the tests. Justify the applied main flow rates taking into consideration the applicable measurement error. Taking into consideration that "for all brine testing, the primary flow rate was set … to follow a predetermined flow rate curve based on decay heat," the justification should substantiate the applicability of the test results on the basis of adequate representation of DH and its uncertainty.

Response

a. The instrument measurement accuracy provided in PWROG-15091-P, Table 5-4 accounts for instrument accuracy and data acquisition system accuracy. One Rosemount flow meter was used to measure the test section outlet flow rate. The instrument accuracy from the manufacturer is ±0.25% of the measurement for the entire span of the instrument. The NI 9203 mA input card used to acquire signals from the Rosemount flow meter has an accuracy of ± 0.04% times the measured current ± 0.0043 mA. The combined accuracy of the flow meter and analog input card reported was calculated using the square root sum of squares (SRSS) of the NI 9203 analog input module and the flow meter sensor accuracy. To simplify the analysis, the analog input module accuracy is evaluated at the instrument span (100 gpm) to be equal to ± 0.062% (0.0004 + 0.0043mA/20mA) of the reading. For flow meter F1, the accuracy is then ± 0.258% of the reading $(0.062^2+0.25^2)^{0.5}$. Since this accuracy was calculated at the instrument span (100 gpm), it bounds the accuracy of the instrument at lower readings. At the maximum flow rate used in the testing (1.3 gpm), the combined accuracy is ± 0.0034 gpm (0.00258*1.3 gpm).

The flow meter was calibrated to within the manufacturer's tolerance, down to 0.390 gpm, by Alden Research Lab prior to its use in the brine test facility.

b. The manufacturer accuracy for the brine injection pump is ±1% of the reading.

c. The inlet flow rate (main flow rate) used in the brine testing was calculated by subtracting the prescribed brine injection flow rate from the measured outlet flow rate:

$$Q_{inlet} = Q_{outlet} - Q_{brine} \qquad \text{Eq. RAI-3.29-1}$$

Both quantities have individual accuracies, as provided in the responses to Items a. and b. The uncertainty in the calculated inlet flow rate can be determined using the square root sum of squares method:

$$\delta Q_{inlet} = [(\delta Q_{outlet})^2 + (\delta Q_{brine})^2]^{0.5} \qquad \text{Eq. RAI-3.29-2}$$

Where δQ_{outlet} is the accuracy of the measured outlet flow rate, and δQ_{brine} is the accuracy of the brine injection flow rate. At the maximum outlet flow rate used in the testing (1.3 gpm), the uncertainty in the calculated inlet flow rate is ±0.006 gpm $(0.0034^2 + 0.005^2)^{0.5}$. Compared to the measured flow rates, the uncertainty in the calculated inlet flow rate due to the flow meter and brine pump accuracy is very small.

The error between the calculated inlet flow rate and the predetermined flow rate is the difference between the two values divided by the predetermined flow rate:

$$E = \frac{Q_{test} - Q_P}{Q_P} \qquad \text{Eq. RAI-3.29-3}$$

Where Q_{test} is the calculated inlet flow rate from the test, and Q_P is the predetermined flow curve based on decay heat. The error is calculated for brine test T029. The measured outlet flow rate, brine injection flow rate, and calculated inlet flow rate from this test are shown in Figure 7-8 of PWROG-15091-P. The predetermined flow curve for this test is Flow Control 2 shown in Figure 5-5 of PWROG-15091-P. The uncertainty associated with the inlet flow rate (±0.006 gpm) is not included in the error calculation since it is small compared to the inlet flow rate. Figure RAI-3.29-1 shows the error between the test inlet flow rate and the predetermined flow curve used in the testing for brine test T029. As the figure shows, the majority of inlet flow data points fall within a range of +20% and -30% of the predetermined flow curve.

Although the error between the calculated inlet flow rate from the brine testing and the predetermined flow curve is not negligible, it is acceptable. As described in the response to RAI-3.28, the brine testing determined the conditions under which a continuous debris bed could not form at the core inlet and represented those conditions in the form of Froude number. In determining the Froude number, the inlet velocity was taken from the test data, and not the

predetermined flow curve. As shown above, the uncertainty associated with the test inlet flow rate is very small (<0.006 gpm) such that the uncertainty in the velocity is small. For example, for an inlet flow rate of 0.8 gpm, the velocity through the Westinghouse bottom nozzle used in the brine testing is 0.0619 ±0.0005 ft/s. The predetermined flow curve based on Appendix K decay heat was used to establish the range of inlet flow rates that was representative of the prototypic large cold leg break scenario, but since the condition under which a continuous debris bed cannot form was determined from the test data, it was not required that the flow rate used in the testing followed the predetermined flow curve with great accuracy.

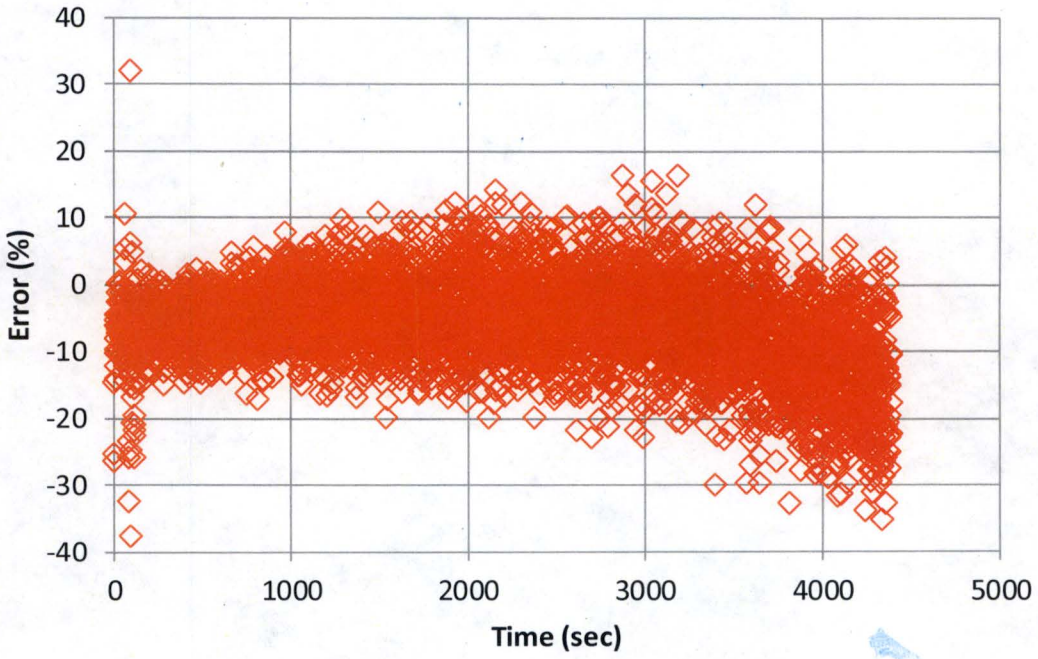

Figure RAI-3.29-1 Error in Brine Test Inlet Flow Rate from Test T029

RAI-3.30

A brine injection flow rate of 0.5 gpm was used in all tests described in PWROG-15091. The source concentration of KBr in the injection solution, while kept constant for each test, was set at several different concentration levels for different tests. Based on the test matrix for the Westinghouse core inlet geometry in Table 6-1, the concentrations were equal to 5, 10, and 15 wt%. As both the rate of fluid injection and the concentration of the solute in the fluid were constant in each individual test, the rate of solute injected into the test column was constant.

The scalability of the tests with regard to time is in question. The relation between the timing in the tests and the timing of the process of solute accumulation in the prototype system is not established in the test report. It is not clear how the real time scale can be transposed relative to the experimental time scale at each source concentration level used in the tests. Provide the scaling basis for the applied process of brine solute injection in the tests so that the relevance of the timing aspect of the observed processes can be related to the behavior of the prototype system.

Response

The design of the subscale facility makes it impossible to scale the tests with regard to time. Instead of simulating a transient condition in which the solute concentration in the core region is continually increasing, the strategy taken for the brine testing is to create a series of steady-state conditions in which buoyancy driven exchange flow will occur in the subscale facility. Figure RAI-3.30-1 shows the control volume defined for the test scenario. As the figure shows, brine will be injected into control volume 1 (V1) several inches above the test section geometry. As the brine concentration builds within V1 a density gradient will develop between V1 and control volume 2 (V2). Once the density gradient is large enough to overcome the upward flow through the flow column, buoyancy driven mass transport will begin.

Prior to starting the brine testing, simulations were performed to help define appropriate boundary and initial conditions for the testing. Applying the transport model discussed in Section 3.3 of PWROG-15091-P to the subscale system shown in Figure RAI-3.30-1, the concentration buildup and exchange flow can be estimated for various brine injection flow rates and concentrations. Figure RAI-3.30-2 shows the predicted concentration buildup in the subscale flow column using a fixed source injection concentration of 20 wt% KBr. Note, a source concentration of 20 wt% KBr was not used in the testing because it was determined that the equivalent boric acid concentration would be near the solubility limit. However, the conclusions drawn from the subscale system analysis discussed here would not change based on the value of the source concentration chosen. Figure RAI-3.30-2 shows the onset of mass transport occurs much earlier compared to the prototypic system prediction shown in Figure RAI-3.30-3. The prototypic system predicts the onset at half an hour while the subscale prediction is before 100 seconds for the four injection flow rates analyzed.

Since the time scale associated with the onset of mass transport between the core region and the lower plenum region of the subscale flow column cannot be preserved, the time at which brine is injected relative to debris was varied within the test matrix. Two brine injection times were chosen. The first

time, concurrent with brine and debris injection, was chosen to represent a condition in which the onset of buoyancy driven convection had occurred consistent with the time of debris arrival. The second time, delayed brine injection, was chosen to represent a condition in which a debris bed had begun to form prior to the onset of buoyancy driven convection.

Figure RAI-3.30-4 shows the exchange flow transient from the prototypic system, predicted from the transport model. The exchange flow begins at zero and increases over time. At 4 hours the exchange flow through the core inlet is approximately 6 lbm/sec. Scaling this value to the subscale geometry results in an exchange flow rate of approximately 0.07 gpm. Figure RAI-3.30-5 shows the estimated exchange flow rate for the subscale geometry with a 20 wt% KBr source injection concentration and various injection flow rates. The figure shows that an injection flow of 0.75 gpm results in an exchange flow rate of approximately 0.07 gpm. Although the exchange flow rate is preserved, it is only for a given point in time for a specific plant condition. For these reasons the source concentrations were varied within the test matrix in order to create a range of exchange flow rates.

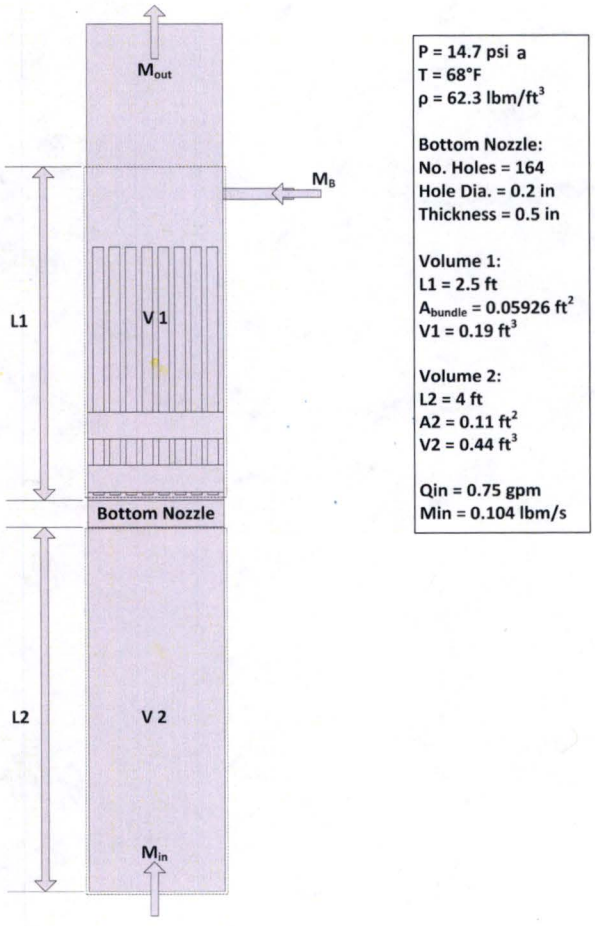

Figure RAI-30.3-1 Subscale Test Facility Control Volume for Brine Testing

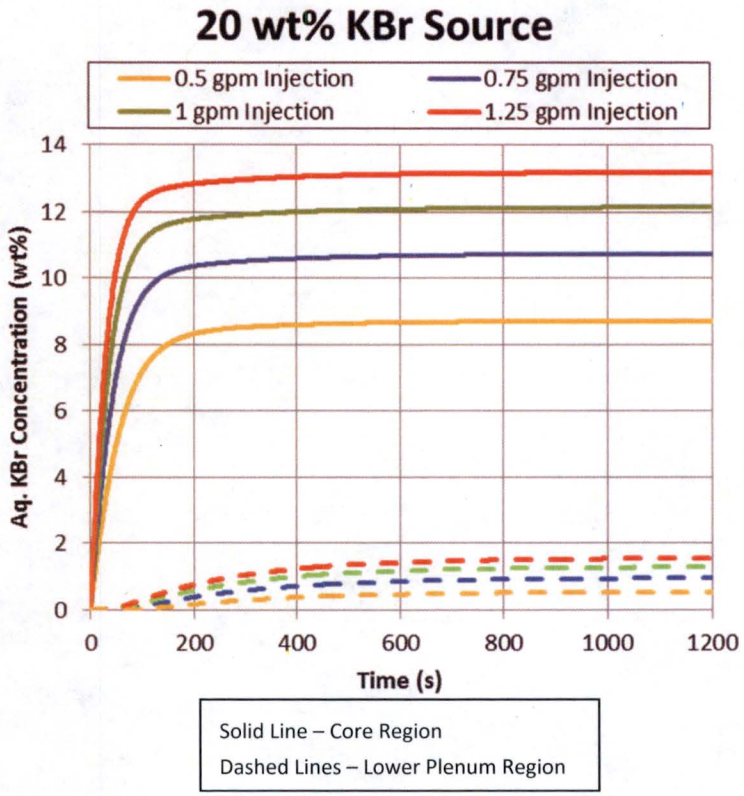

Figure RAI-3.30-2 Estimated Concentration Buildup in Brine Test

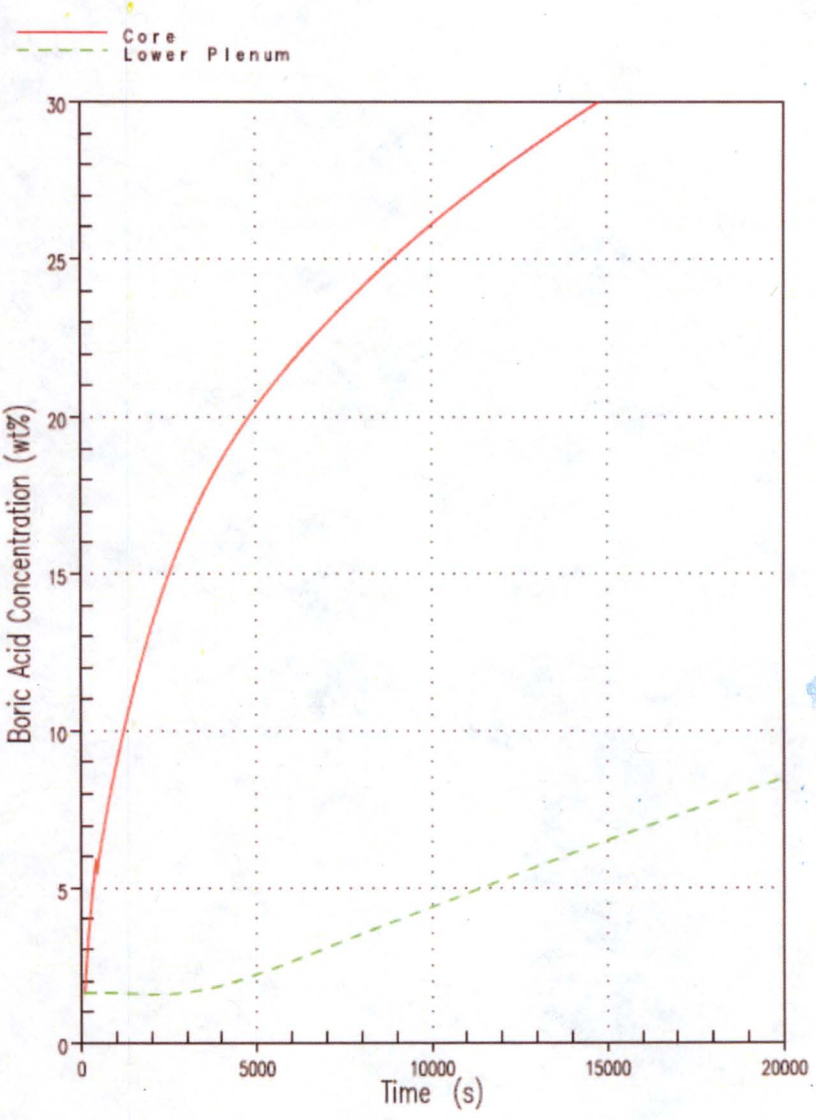

Figure RAI-3.30-3 Predicted Boric Acid Concentration Build-Up from Boron Transport Model

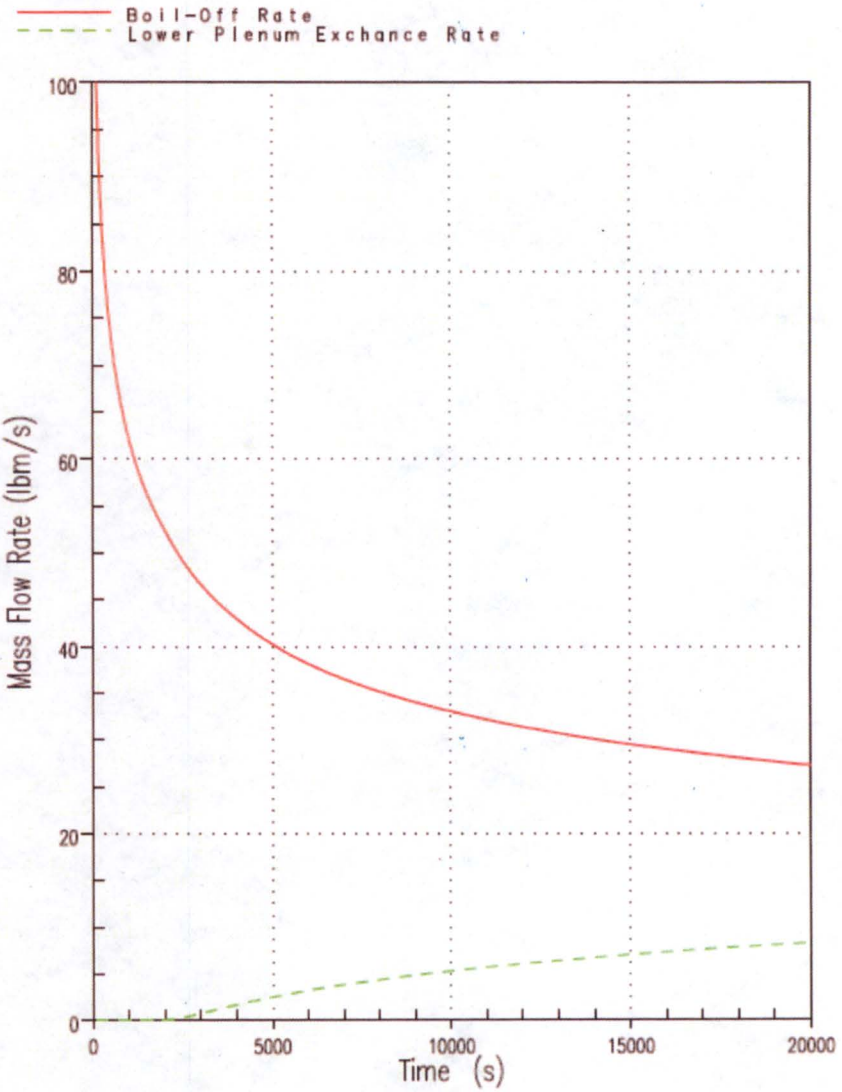

Figure RAI-3.30-4 Boil-off Rate Compared to the Core-to-Lower Plenum Exchange Flow Rate Predicted by the Boron Transport Model

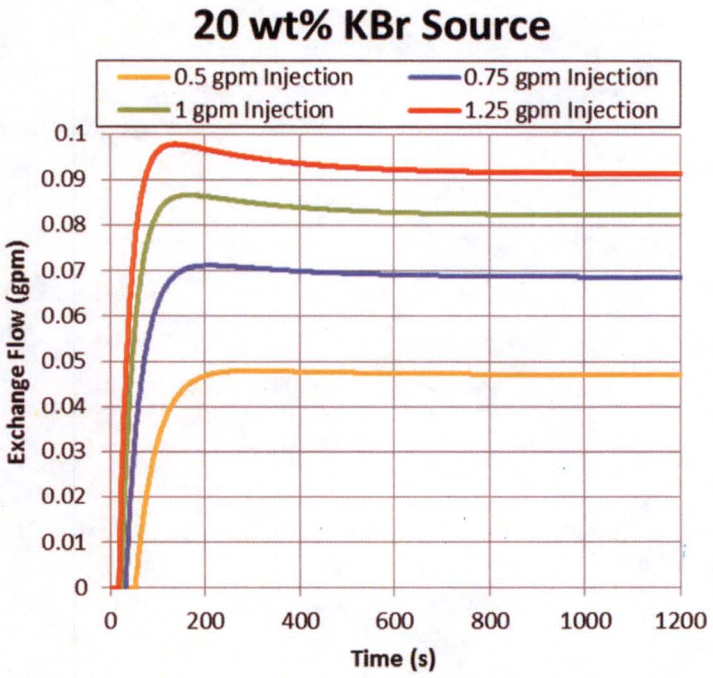

Figure RAI-3.30-5 Estimated Exchange Flow in Brine Test

RAI-3.31

Section 5.3 in PWROG-15091 describes the sparger pipe used for injecting the brine solution into the test section. The resulting average fluid exit velocity at the applied brine injection rate of 0.5 gpm was 0.97 feet per second (ft/sec) (29.5 centimeters per second). Based on the sketch in Figure 5-14, the holes were located along the axial length of the sparger so that the flow velocity through the hole(s) farthest from the blocked end of the sparger should have been noticeably larger than the average injection velocity of 0.97 ft/sec.

Section 5.3 explains that a brine solution injection velocity of 1.94 ft/sec corresponding to an injection rate of 1 gpm "is sufficient to induce mixing in the subscale core region but is low enough to minimize any impact on the buoyancy-driven process being studied." Section 7.1, describing the pressure response observed in the tests, states in part that 'the pressure trends seen throughout the test program include a small pressure spike corresponding to the start of brine injection…" Figure 7-2 shows the pressure record for TestT021 with delayed brine injection, which is described "typical" for all tests with delayed brine injection. The initiation of brine injection caused a significant jump of about 3 pounds per square inch (psi) gauge in the system pressure. Presumably, the measurement was taken from the upstream pressure transducer, shown in Figure 5-1, which had an accuracy of plus or minus 0.289 psi based on Table 5-4. A similar effect is also seen in Figure 7-1 for Test T029 with no brine injection delay.

Provide justification that jetting did not have an impact on the test results including the timing of the testing observations. Justify that the major findings from the tests relevant to WCAP-17788 are not affected.

Response

Shakedown testing was performed for two different sparger hole sizes and orientations. The first sparger design utilized 6 holes all with a diameter of 3/16 inches. Upon testing this design it was observed that the brine distribution through the holes was not uniform. As a result, the hole diameters were adjusted to correct for this effect. The revised design utilized holes that progressively get smaller in 1/32 inch increments to create a more uniform brine injection. Visual inspection during shakedown testing confirmed that the brine injection is uniform across the flow area of the test section.

With regard to sparger orientation, two different orientations were considered. The first orientation had the sparger holes pointing downward while the second had the sparger holes pointing upward. Testing showed that regardless of orientation, the brine distribution and transport rates were comparable and independent of sparger design as shown in Figure RAI-3.31-1. Regardless of this outcome, the orientation with the sparger holes pointing upward was chosen to ensure that any inertia due to the injection will not influence the transport process at the core inlet or disrupt the debris bed.

As shown in PWROG-15091-P, Figures 7-1 and Figure 7-2, the test column pressure increases when the brine injection is initiated. There was a concern that this pressure spike would influence the debris bed that had formed prior to the start of brine injection in the delayed brine injection tests. This is only a

concern in the delayed brine injection tests since a debris bed had not formed in the tests conducted without brine injection delay.

During the delayed brine injection tests, the debris bed was observed closely to visually determine if the initialization of brine injection led to any change to the debris bed. In all the brine injection tests, no change in the debris bed was observed when the brine injection was started. The pressure drop measured across the debris bed was also monitored when brine injection was initiated. No significant changes in the measured pressure drop were noted.

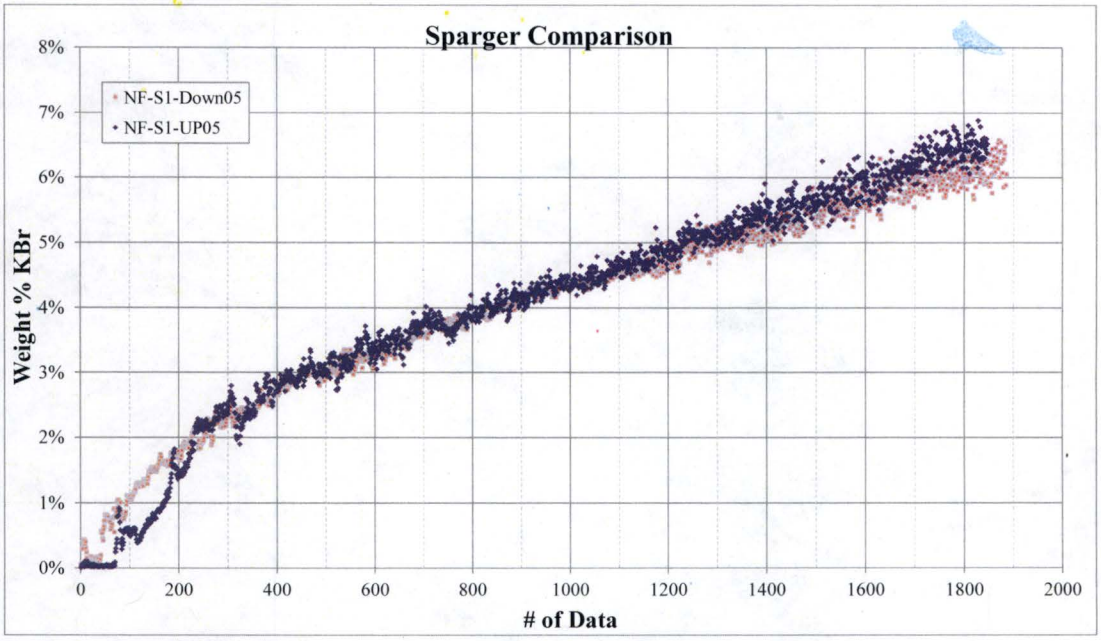

Figure RAI-3.31-1 Comparison of KBr Concentration below Core Inlet following Injection from the Two Sparger Orientations (Holes Pointing Down vs. Holes Pointing Up)

RAI-3.32

Section 3.5 "Equations," explains that the equations for calculating the amount of fiber delivered to the core inlet are solved explicitly as a difference from time step to time step and that they can be easily solved by hand. In addition, Section 3.5.8, "Suggested Time Step Interval," states in part that "for this evaluation, a time step of one minute is suggested."

Section 6.5 of Volume 1, Subsection 6.5.2.1, "Time Step," also discusses time steps for the hot leg break (HLB) methodology. The HLB method states that an iterative solution with respect to time is necessary and recommends that time step sensitivity be performed. The method suggests that the time step should be small enough to ensure that the important processes behave linearly over each time step. A starting time step value of 100 seconds is recommended.

a. Provide results for an example case analyzed with the CLB method to illustrate the effect of the time step size. Provide the results from two calculations performed with time step sizes of 1 second and 10 seconds and compare the results from the calculation using the recommended time step size of 60 seconds.
b. Provide results for an example case analyzed with the HLB method to illustrate the effect of the time step size. Provide the results from two calculations performed with time step sizes of 1 second and 10 seconds and compare the results from the calculation using the recommended time step size of 100 seconds.
c. Provide quantitative criteria for assuring that the results from a calculation performed with both the CLB and HLB methods produce "stable results" along with justification as to how these criteria will be assured. State how the proposed process assures that an appropriate time step size will be applied to the proposed methods.

Response

a. The response to this question is provided in the WCAP-17788, Volume 3 RAI response.

b. WCAP-17788, Volume 1, Section 6.5 describes the method for calculating a fiber limit following a hot leg break (HLB) for any given plant. This methodology provides an analytical solution to the fiber distribution throughout the system. Because of this, errors are not introduced with each time step as they would be in a numerical solution where the differential equations are approximated. This means that the time step is not as important as it is in many thermal-hydraulic (TH) codes. While the time step does not affect the solutions to the equations, it is necessary for two other reasons: capturing the time dependent boundary conditions such as hot leg switchover and checking the stopping criteria. For both of these needs, the time step should be small enough such that these important events are not missed by a significant amount of time.

   WCAP-17788, Volume 1, Section 6.5.6 provides two example calculations for the HLB methodology. As stated therein, these cases can be used to verify an implementation of this methodology. However, the inputs for these cases are not intended to reflect realistic plant

conditions; rather, they are intended to test implementation of the methodology. To that end, generic time step sensitivity studies of the nature requested would be of little value.

Therefore, it is recommended that each utility perform a time-step sensitivity study as part of their analysis. This process would include selecting a base time step of 100 seconds as described in Section 6.5.2.1 of WCAP-17788, Volume 1. Additional cases should be run in which this time step is varied until it can be demonstrated that the time step used is stable. Stability would be demonstrated by a change of less than one percent in the final results.

c. The acceptability of the time step was addressed in the WCAP-17788, Volume 3 RAI response.

As described in the response to Item (b) of this RAI, generic time step sensitivity studies of the nature requested for the hot leg break method are of little value. For plant-specific applications, it is recommended that each utility perform a time-step sensitivity study as part of their analysis. This process would include selecting a base time step of 100 seconds as described in Section 6.5.2.1 of WCAP-17788, Volume 1. Additional cases should be run in which this time step is varied until it can be demonstrated that the time step used is stable. Stability would be demonstrated by a change of less than one percent in final results.

Proposed Revision to Volume 1:

Given the above response, WCAP-17788, Volume 1, Section 6.5.2.1 is revised and expanded to read as follows:

6.5.2.1 Time Step

Because this problem contains time varying boundary conditions, specifically the core inlet resistance and ECCS configuration, an iterative solution with respect to time is necessary.

Time step sensitivity should be performed in order to demonstrate stable results calculated by the chosen time step. The time step should be small enough such that the important processes, namely the injection of fiber, do not change by more than 1% as a result of a change in time step. A starting value of 100 seconds is recommended.

RAI-3.33

Section 7 in Volume 1 states that the subscale brine test program documented in PWROG-15091 "considered both Westinghouse and AREVA core inlet geometries by using prototypic fuel components." Provide the following clarifying information regarding the test rig geometry.

a. Explain how the value of [ ], provided in: Table 5-2 in PWROG-15091 for the ratio of test column inlet flow area to installed FA inlet flow area, was calculated (the value differs from the open flow area ratio of [ ] in the same table, which is based on the flow area of [ ] holes).

b. Table 5-2 pertains to the tests for the Westinghouse bottom nozzle. Provide a similar table for the tested AREVA fuel nozzle.

c. For both tested fuel geometries, provide the distance between the test column wall inner surface and the closest point on the surface of the peripheral fuel rod elements for all four sides of the square test column. In addition, provide the fuel rod pitch and the fuel assembly pitch for each fuel assembly as well as the types of the prototypical fuel assemblies considered (e.g., 17x17).

d. Was the gap between the peripheral fuel rods and the column wall measured and controlled during the test program? It appears from Figure 5-9 in PWROG-15091 that the gap on the "west" side of the depicted square is larger than the gaps on the remaining three sides (due to the location of the thimble tubes). Provide the flow area in the fuel bundle test region (Figure 9-11 in Volume 1) and the corresponding flow area of the represented region of the fuel bundle. Provide information for both Westinghouse and AREVA tests fuel bundles.

e. Provide assurance that the test findings using the tested fuel bundle geometries remain valid for other fuel types.

Response

a. The ratio of [ ]^{a,c} is based on the bottom nozzle flow area of [ ]^{a,c} compared to the total test column flow area (excluding fuel) of [ ]^{a,c} The ratio of [ ]^{a,c} is based on the test column cross-sectional flow area of [ ]^{a,c} compared to the total assembly flow area (excluding fuel) of [ ]^{a,c} based on a fuel assembly pitch of [ ]^{a,c}

b. Table RAI-3.33-1 shows the important dimensions of the tested lower end fitting **FUELGUARD™**.

FUELGUARD is a trademark or registered trademark of AREVA. Other names may be trademarks of their respective owners.

Table RAI-3.33-1 Summary of Tested AREVA Bottom Nozzle FUELGUARD

	Value	Units
Flow Openings	[ ]a,c	in
Total open flow area	[ ]	in^2
Test column flow area	[ ]	in^2
Open flow area ratio	[ ]	%
Ratio of test column inlet flow area to installed FA inlet flow area[1]	[ ]	%
Note 1: This value is used to scale results from the test geometry to a full-area fuel assembly.		

c. The following gaps between the rods and the wall are given in reference to Figure 3-23 of WCAP-17788 Volume 6, re-presented below as Figure RAI-3.33-1. The grid strap in the center of the image is centered at 2 in. in a 4 in. channel. The fuel rod diameter of [ ]^{a,c} and fuel rod pitch of [ ]^{a,c} results in a gap of [ ]^{a,c} The gap on the left side, determined by the thimble tubes with a diameter of [ ]^{a,c}, is [ ]^{a,c} The remaining fuel information requested is in Table 3-3 of WCAP-17788 Volume 6.

d. The gaps were not measured. During the test program, visual inspection was performed to ensure the rods were not touching the walls. The design of the assembly insert also assured control of the gap space. Indeed, the gaps on the "west" side of the housing that had the thimble tubes were smaller, as the thimble tubes have a larger OD than the fuel rods. The flow area in the fuel bundle (excluding grids) for both fuel types is [ ]^{a,c}

e. The brine testing was completed in order to demonstrate that buoyancy driven convection due to density gradients between the core and lower plenum regions is an effective process for disrupting debris bed formation at the core inlet. For buoyancy driven convection to occur, the potential force created by the density gradient must be strong enough to overcome the upward flow of liquid from the lower plenum into the core region. The fuel bottom nozzle geometries tested were selected because they have the smallest flow areas and therefore bound all other fuel bottom nozzles. The bottom nozzle geometries used for the brine testing are the same as those used in the subscale head loss final limits testing documented in WCAP-17788 Volume 6. These geometries were used in the final limits head loss testing because they have the smallest flow areas and therefore bound all other fuel bottom nozzles. Buoyancy driven convection through

bottom nozzle designs with larger flow areas would be increased, for the same density gradient, since the flow velocity through these bottom nozzle designs would be less.

a,c

Figure RAI-3.33-1 Test Section Top View Showing Bottom Nozzle Flow Holes with Respect to Simulated Fuel Rods

RAI-3.34

Provide a sectional breakdown of PWROG-15091-P, listing the sections unrelated to the review and approval of WCAP-17788. Also list those sections needing review by the U.S. Nuclear Regulatory Commission (NRC) and explain how that determination was made. Provide any additional clarification to aid the NRC staff in the review.

Response

In the supplement of WCAP-17788 Volume 1, a number of processes are identified that preclude uniform debris accumulation at the core inlet. The brine test report is referenced to demonstrate that one of the processes (i.e., buoyancy-driven countercurrent exchange flow) that generate secondary flows at the core inlet is sufficient to preclude uniform debris bed formation at the fuel inlet. Secondary flows, driven by processes like buoyancy-driven exchange flow, create circulation patterns and flow oscillations at the core inlet that lead to non-uniform debris accumulation. The intent of the brine testing is to provide a demonstration that the buoyancy-driven process is sufficient to preclude uniform debris accumulation.

The Brine Test Program Report, PWROG-15091-P, is a comprehensive test report that includes a review of previous buoyancy-driven exchange flow work, a description of the test facility design and operation, the test matrix, an overview of the test results, data analysis, model development and predictions, and conclusions. Since this report is not being reviewed by the NRC staff for approval, only certain aspects of the brine test report need to be considered. Since conclusions from the summary of previous works are not considered in the supplement of WCAP-17788 Volume 1, NRC review of Section 3 of the report is not necessary. Further, any discussion related to model development and predictions contained in Sections 9, 10, and 11 do not require approval since the supplement of WCAP-17788 Volume 1 relies solely on the test observations and conclusions contained in the brine test report.

Provided below is the Table of Contents (TOC) for PWROG-15091-P. Sections deemed by the PWROG to be unrelated to the review and approval of WCAP-17788 are struck-through. The sections not struck-through are related to the test facility design and operation, test matrix, test results, and conclusions. The PWROG believes that NRC review of these sections is sufficient to conclude that the brine testing is adequate to demonstrate that buoyancy-driven countercurrent exchange flow is capable of precluding uniform debris accumulation at the core inlet under prototypic CLB conditions, which is the key piece of information referenced by WCAP-17788.

TABLE OF CONTENTS

WCAP-17788-NP Mark-ups

Proposed revisions to WCAP-17788-NP, Volume 1 are included in this section. After receipt of the Final Safety Evaluation, the NRC Approved version of the TR will incorporate the proposed revisions. Revisions are identified with revision bars in the left margin. Deleted text is identified as blue font with a single strikethrough and new text is identified as red font.

Proposed revisions to the TR are summarized as follows:

- WCAP-17788-NP, Volume 1 pg. 6-28: Updates to the text are made consistent with the response to RAI-3.32.

12. Time of HLSO and Resulting Flow Splits

6.5.2.1 Time Step

Because this problem contains time varying boundary conditions, specifically the core inlet resistance and ECCS configuration, an iterative solution with respect to time is necessary.

Time step sensitivity should be performed in order to demonstrate stable results calculated by the chosen time step. The time step should be small enough such that the important processes, namely the injection of fiber, do not change by more than 1% as a result of a change in time step~~behave linearly over each time step~~. A starting value of 100 seconds is recommended.

6.5.2.2 Plant Type

The values for t_{block} as well as the correlations used to calculate K_{split} and m_{split} are dependent on plant type, as described in Section 6.1. Therefore, the plant design must be identified. The plant types of interest for this analysis are:

1. B&W Design
2. Westinghouse Upflow BB Design
3. Westinghouse Downflow BB Design
4. CE Design

6.5.2.3 Fuel Vendor

The core inlet head loss with debris is dependent on fuel vendor, as described in Section 6.3. Therefore, the fuel vendor must be identified. The fuel vendors of interest for this analysis are:

1. AREVA
2. Westinghouse

6.5.2.4 Number of Fuel Assemblies

The total number of fuel assemblies is used to calculate the value of K_{split}, as described in Step 6 of Section 6.5.3. This value is fixed for each plant and therefore does not need to be parameterized.

6.5.2.5 Initial Sump Fiber Load

The initial sump fiber load is plant dependent and should bound the largest total sump fiber load 30 days after event initiation. This fiber load consists only of the fiber fines in the sump, not the total of all fiber, as described in Section 3.5.